© 2014. Published by The Company of Biologists Ltd | Development (2014) 141, 28-38 doi:10.1242/dev.097295

RESEARCH ARTICLE

STEM CELLS AND REGENERATION

Meis2 is a Pax6 co-factor in neurogenesis and dopaminergic periglomerular fate specification in the adult olfactory bulb

Zsuzsa Agoston[1,2,*,], Peer Heine[2,‡,**], Monika S. Brill[3,4,§,**], Britta Moyo Grebbin[1], Ann-Christin Hau[1], Wiebke Kallenborn-Gerhardt[2,¶], Jasmine Schramm[1], Magdalena Götz[3,4] and Dorothea Schulte[1,2,‡‡]**

ABSTRACT

Meis homeodomain transcription factors control cell proliferation, cell fate specification and differentiation in development and disease. Previous studies have largely focused on Meis contribution to the development of non-neuronal tissues. By contrast, Meis function in the brain is not well understood. Here, we provide evidence for a dual role of the Meis family protein Meis2 in adult olfactory bulb (OB) neurogenesis. Meis2 is strongly expressed in neuroblasts of the subventricular zone (SVZ) and rostral migratory stream (RMS) and in some of the OB interneurons that are continuously replaced during adult life. Targeted manipulations with retroviral vectors expressing function-blocking forms or with small interfering RNAs demonstrated that Meis activity is cell-autonomously required for the acquisition of a general neuronal fate by SVZ-derived progenitors *in vivo* and *in vitro*. Additionally, Meis2 activity in the RMS is important for the generation of dopaminergic periglomerular neurons in the OB. Chromatin immunoprecipitation identified doublecortin and tyrosine hydroxylase as direct Meis targets in newly generated neurons and the OB, respectively. Furthermore, biochemical analyses revealed a previously unrecognized complex of Meis2 with Pax6 and Dlx2, two transcription factors involved in OB neurogenesis. The full pro-neurogenic activity of Pax6 in SVZ derived neural stem and progenitor cells requires the presence of Meis. Collectively, these results show that Meis2 cooperates with Pax6 in generic neurogenesis and dopaminergic fate specification in the adult SVZ-OB system.

KEY WORDS: Pax6, TALE-homeodomain proteins, Adult neurogenesis, Subventricular zone, Mouse

INTRODUCTION

The subventricular zone (SVZ), located between the lateral ventricle and the striatum, and the subgranular zone (SGZ) of the dentate gyrus of the hippocampus are major stem cell niches in the adult mammalian brain. Adult neural stem cells exhibit astroglial characteristics, proliferate slowly and produce an intermediate population of fast dividing progenitor cells (transient amplifying progenitors, TAPs), which in turn give rise to neuroblasts. Neuroblasts express traits of immature neurons such as neuron-specific class III β-tubulin (TuJ1; also known as Tubb3), the polysialylated form of neural cell adhesion molecule (PSA-NCAM) or the microtubule-associated protein doublecortin (Dcx). SVZ-born neuroblasts migrate in chains along the rostral migratory stream (RMS) towards the olfactory bulb (OB), where they differentiate into a wide variety of phenotypes, including GABAergic granule cells (GCs) in the granule cell layer (GCL), glutamatergic juxtaglomerular neurons and periglomerular interneurons (PGNs) in the glomerular layer (GL). The latter are further classified as either dopaminergic, calbindin-expressing or calretinin-expressing cells (Parrish-Aungst et al., 2007). These diverse populations of OB neurons originate from distinct regions within the SVZ or RMS (Hack et al., 2005; Merkle et al., 2007; De Marchis et al., 2007). In fact, SVZ-derived stem and progenitor cells largely retain their regionally pre-specified differentiation potential after heterotopic transplantation (Merkle et al., 2007). Cell-intrinsic mechanisms, including the differential expression of transcriptional regulators, are therefore of particular importance for neuronal subtype specification in the SVZ-OB neurogenic system. The exact nature of these intrinsic determinants is just beginning to be elucidated. The paired-type transcription factor Pax6 and the distal-less transcription factor Dlx2, for instance, together instruct a dopaminergic/GABAergic fate, the zinc-finger transcription factor Sp8 is required for the generation of calretinin-expressing PGNs, whereas glutamatergic interneurons derive from progenitors expressing neurogenin 2 or Tbr2 (also known as Eomes) (Brill et al., 2009; Brill et al., 2008; Hack et al., 2005; Hsieh, 2012; Kohwi et al., 2005; Kohwi et al., 2007; Waclaw et al., 2006). These and other studies have led to the view that migrating neuroblasts express defined combinations of transcription factors, which reflect particular lineage restrictions.

Meis1-3 belong to the TALE (three amino acid loop extension) class of atypical homeodomain (HD)-containing transcription factors, which are characterized by three extra amino acids between helix 1 and helix 2 of the homeodomain. They form heteromeric complexes with other transcriptional regulators, including the related PBC family, members of the Hox clusters or basic helix-loop-helix (bHLH) proteins (Chang et al., 1997; Knoepfler et al., 1999; Moens and Selleri, 2006; Moskow et al., 1995). Meis proteins regulate cell cycle kinetics and cell fate specification of distinct progenitor cells and control various developmental processes, including limb, heart, retina and brain development (Agoston and Schulte, 2009; Agoston et al., 2012; Bessa et al., 2008; Choe et al., 2009; Heine et al., 2008; Hisa et al., 2004; Mercader et al., 1999; Paige et al., 2012; Vitobello et al., 2011). In the hematopoietic system, Meis1, along with Pbx and Hox proteins, is essential for the correct balance between self-

[1]Institute of Neurology (Edinger Institute), J. W. Goethe University Medical School, D-60528 Frankfurt, Germany. [2]Department of Neuroanatomy, Max-Planck-Institute for Brain Research, D-60528 Frankfurt, Germany. [3]Physiological Genomics, Institute for Physiology, Ludwig-Maximilians University Munich, D-80336 Munich, Germany. [4]Institute for Stem Cell Research, Helmholtz Zentrum München, D-85764 Neuherberg, Germany.
*Present address: Department of Pharmacology, Howard Hughes Medical Institute, and Institute for Stem Cell and Regenerative Medicine, University of Washington School of Medicine, Seattle, WA 98109, USA. ‡Present address: Maxcyte Inc., Gaithersburg, MD 20878, USA. §Present address: Institute of Neuronal Cell Biology (TUM-NCB), Technical University Munich, D-80802 Munich, Germany. ¶Present address: pharmazentrum frankfurt/ZAFES, Institute of Clinical Pharmacology, Frankfurt University Medical School, D-60590 Frankfurt, Germany.
**These authors contributed equally to this work

‡‡Author for correspondence (dorothea.schulte@kgu.de)

Received 8 April 2013; Accepted 3 October 2013

Development (2014) doi:10.1242/dev.097295

renewal and maturation of primitive progenitors. Furthermore, Meis1 dysregulation is a frequent occurrence in MLL-induced leukemia, implicating Meis family proteins in hematopoietic stem and progenitor cell activity in the adult under physiological and pathophysiological conditions (Calvo et al., 2001; Nakamura et al., 1996; Wong et al., 2007). Expression of Meis2 in the adult SVZ, OB and in SVZ-derived neuroblasts has been observed, but if and how Meis2 contributes to adult SVZ neurogenesis is still unknown (Allen et al., 2007; Marei et al., 2012; Parmar et al., 2003; Pennartz et al., 2004). Here, we provide experimental evidence that Meis2 functions as an essential Pax6 co-factor in adult SVZ neurogenesis and identify Dcx and tyrosine hydroxylase as direct Meis2 targets in this system.

RESULTS

Meis2 is expressed in the SVZ, RMS and distinct neuronal populations of the OB

We first assessed *Meis2* expression in 5- to 7-week-old mice. Strong *Meis2* transcript expression was visible in the RMS and the dorsal/lateral walls of the lateral ventricle (Fig. 1A-E; supplementary material Fig. S1). Prominent expression was also seen in the OB, with high levels in the GCL and in dispersed cells in the GL (Fig. 1B,F). Notably, the dentate gyrus of the hippocampus was devoid of *Meis1* or *Meis2* specific transcripts and protein (Fig. 1G,H; supplementary material Fig. S1; data not shown). In agreement with published data, we detected transcripts specific for the paired type transcription factor *Pax6* in the SVZ, RMS and in some OB neurons (supplementary material Fig. S1) (Hack et al., 2005). On the cellular level, we did not detect strong Meis2 protein expression in Gfap-positive cells, including neural stem cells (NSCs) and astrocytes of the SVZ and RMS, or in rapidly proliferating, Ascl1 (Mash1)-expressing TAPs (Fig. 1I-K). By contrast, 97.7% (±1.6% s.d.) of all neuroblasts, which can be recognized by antibodies directed against neuron-specific class III β-tubulin (TuJ1), PSA-NCAM or Dcx, were strongly Meis2 immunoreactive (Fig. 1I-L; data not shown). Consistent with the prominent expression of Pax6 in neuroblasts, we found extensive colocalization of Meis2 and Pax6 in migrating neuroblasts of the SVZ, RMS and the inner part of the OB (Hack et al., 2005) (Fig. 1L; Fig. 2G). The few neuroblasts that were negative for Meis2 may represent Tbr1- or Tbr2-expressing neuroblasts, which are fated to generate glutamatergic, juxtaglomerular neurons (Brill et al., 2009).

In the OB, the vast majority of granule cells were labeled with the Meis2-specific antibody as well as ~60% of the PGNs, whereas Gfap-expressing astrocytes were Meis2 negative (Fig. 2A,A′). Among the three major neurochemically distinct populations of PGNs, 94.4% (±3.09%) of the dopaminergic neurons (identified by their expression of tyrosine hydroxylase, Th) expressed Meis2 (Fig. 2B,E), as did 62.9% of the calbindin-positive neurons (±2.1%; Fig. 2C,E) and 28.3% of the calretinin-positive cells (±1.4%; Fig. 2D,E). Neurogenin 2-expressing cells in the OB, including mitral cells, did not label for Meis2 (Fig. 2F). Dopaminergic fate specification in the OB requires the concerted activities of Pax6, which is almost exclusively expressed in dopaminergic PGNs in the OB, and of the homeodomain protein Dlx2, which is co-expressed with Pax6 in dopaminergic PGNs but also present in granule cells and in a subpopulation of calbindin-positive PGNs (Brill et al., 2008; Hack et al., 2005). Consistently, 83.5% (±2.5%) of all Pax6+ PGNs also expressed Meis2 and the immunoreactivity for Meis2 and a pan-Dlx antibody recognizing all Dlx family proteins,

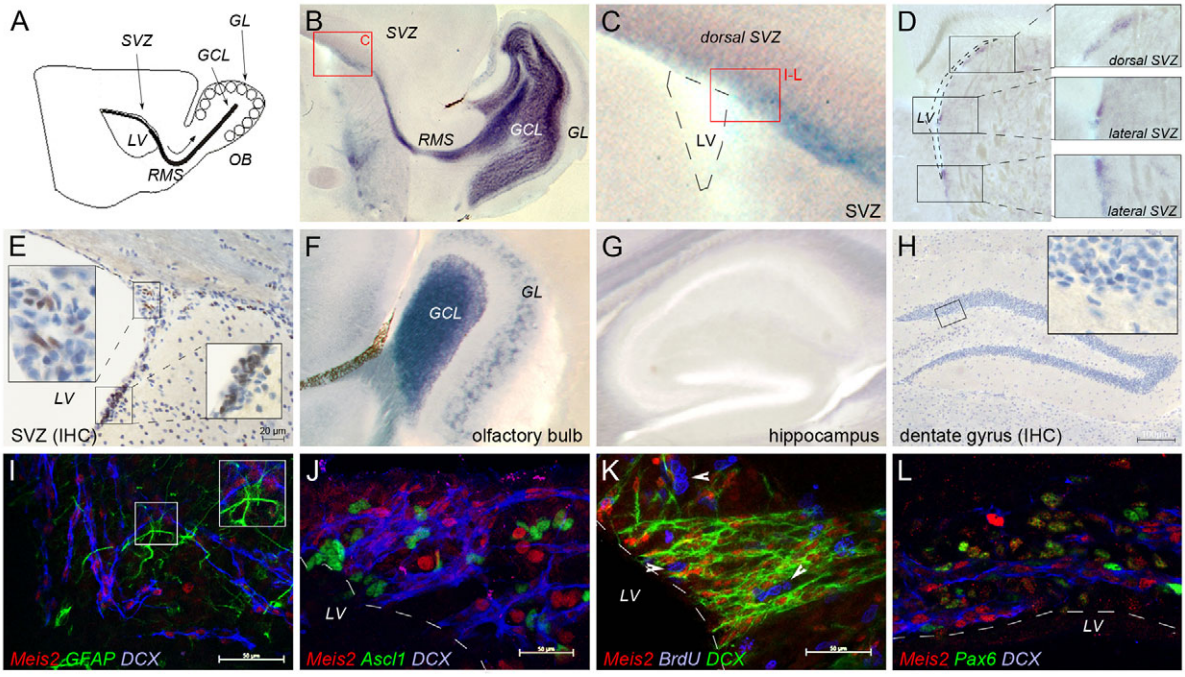

Fig. 1. *Meis2* expression in the adult mouse SVZ and RMS. (A) Schematic of the adult mouse SVZ-RMS-OB system. (B-D,F,G) Meis2 transcript expression in 5- to 7-week-old C57/BL6 mice. (B) Sagittal vibratome section showing Meis2 expression in the SVZ, RMS and OB; (C) SVZ; (D) coronal section showing Meis2 transcripts in the dorsal and lateral SVZ; (F,G) sagittal section of the OB (F) and HC (G). (E,H) Immunohistochemical labeling of coronal sections through the SVZ (E) and HC (H); Meis2 staining is shown in brown, cell nuclei are counterstained with Hematoxylin in blue. (I-L) Co-immunolabeling for Meis2 in the SVZ. (I) Meis2 (red), Gfap (green), Dcx (blue); (J) Meis2 (red), Ascl1 (green), Dcx (blue); (K) Meis2 (red), Dcx (green) and BrdU pulse-labeled cells (blue) in the emerging RMS, arrowheads mark BrdU pulse-labeled TAPs; (L) co-expression of Meis2 (red) and Pax6 (green) with Dcx (blue) in the SVZ. C is a higher magnification of the boxed area in B. The region shown in I-L is marked by the red box in C. GCL, granule cell layer; GL, glomerular layer; HC, hippocampus; LV, lateral ventricle; OB, olfactory bulb; RMS, rostral migratory stream; SVZ, subventricular zone. Scale bars: 100 µm in H; 50 µm in I-K.

Development (2014) doi:10.1242/dev.097295

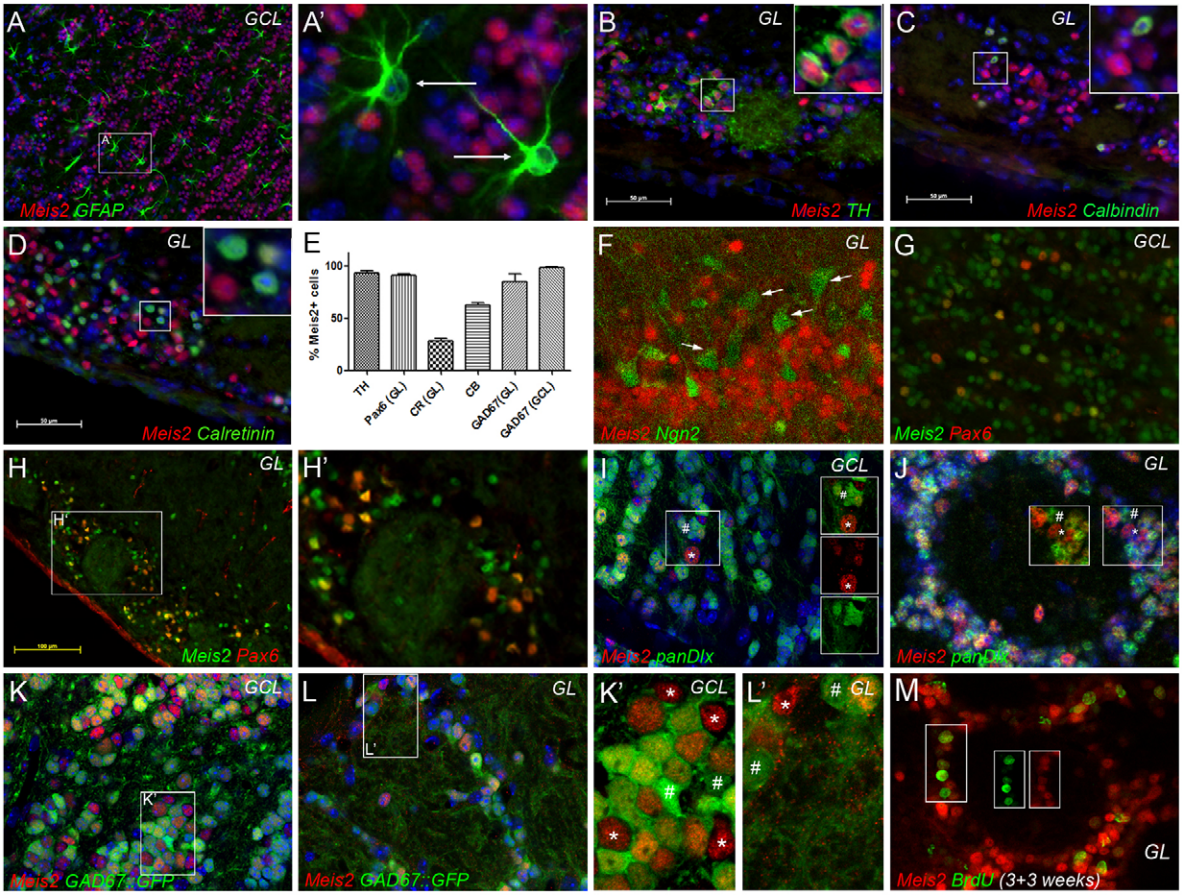

Fig. 2. Meis2 expression in the adult mouse olfactory bulb. (A,A′) Meis2 protein expression in the GC; the arrows in A′ point to Gfap-positive, Meis2-negative astrocytes. (B-D) Subtype-specific Meis2 expression in PGNs; Meis2 is in red. (B) Th (green); (C) calbindin (green); (D) calretinin (green). (E) Relative proportion of Meis2-expression among different PGN subtypes. Error bars represent s.e.m. (F) Lack of co-expression of Meis2 (red) and neurogenin 2 (Ngn2, also known as Neurog2; green). Arrows indicate putative mitral cells, which are immunonegative for Meis2. (G-H′) Meis2 (green) and Pax6 (red) in the GCL (G) and GL (H,H′); all Pax6-immunoreactive PGNs and migrating neuroblasts in the GCL are labeled for Meis2. (I,J) Meis2 (red) and Dlx proteins (panDlx antibody, green) in the GCL (I) and GL (J). (K-L′) Partial co-expression of Meis2 (red) and Gad67 (green) in the GCL (K,K′) and GL (L,L′) of a GAD67::GFP transgenic mouse; asterisks indicate cells single labeled for Meis2, hash symbols indicate cells single labeled for panDlx (I,J) or Gad67 (K′,L′). (M) Meis2 (red), BrdU (green) after 3 weeks of continuous BrdU labeling followed by a 3-week recovery period. A,B-D,I-L were counterstained with DAPI (blue). The boxed areas in A-D,H,I-L are shown at higher magnifications in inserts or as separate panels (A′,H′,K′,L′). The cells in the larger boxed area in M are shown in separate channels in the two smaller boxed areas in M. Scale bars: 50 µm in B-D; 100 µm in H.

including Dlx2, largely overlapped (Fig. 2H-J). Our data thus correspond well to a previous study (Allen et al., 2007) and suggest that dopaminergic PGN specification may broadly require Meis2. In a GAD67::GFP mouse line, which expresses enhanced green fluorescent protein (GFP) under the control of glutamic acid decarboxylase (GAD) 67 (Gad1 – Mouse Genome Informatics) (Tamamaki et al., 2003), most GAD67::GFP-positive cells were labeled for Meis2 (Fig. 2K-L′). To test if Meis2 immunoreactive cells are replaced during adult life, we labeled newly generated OB neurons by continuous application of BrdU in the drinking water for three weeks followed by a three-week differentiation period. Nearly all BrdU-labeled neurons in the GCL and ~60% of all newly generated PGNs were Meis2 positive (Fig. 2M; data not shown). This correlates well with the overall distribution of Meis2-expressing neurons within these cell populations.

Meis activity is required for neurogenesis of adult neural stem and progenitor cells *in vitro* and *in vivo*

Adult stem and progenitor cells of the SVZ can be propagated as neurospheres *in vitro* in the presence of Egf and Fgf2 and differentiate into neurons, astroglia or oligodendrocytes upon growth factor withdrawal (Reynolds and Weiss, 1992). When SVZ-derived neurospheres were differentiated, strong nuclear Meis2 staining was specific for young, TuJ1- and Dcx-positive neurons (Fig. 3A,B). By contrast, Gfap-expressing astrocytes and O4-positive oligodendrocytes, which can be detected in the cultures after seven days of differentiation by their expression of the O4 antigen, did not exhibit strong Meis2 immunoreactivity (Fig. 3C,D). To test if Meis2 expression was required for neuronal differentiation, we reduced Meis expression by small interfering RNA (siRNA)-mediated knockdown (Fig. 3E-H). Because TALE proteins share high sequence similarity and frequently function redundantly, we co-transfected siRNAs targeting *Meis1* and *Meis2* to exclude possible compensation between the two proteins (Azcoitia et al., 2005; Capellini et al., 2006). Efficient Meis protein knockdown was confirmed by western blot (Fig. 3E). Two days after growth factor withdrawal, cells transfected with control siRNA molecules had generated 9.1% neurons and 35.5% astroglia. Upon Meis knockdown however, the number of neurons decreased to 2% (Fig. 3F-H). The few TuJ1-positive cells present in *Meis1/2* siRNA-

Development (2014) doi:10.1242/dev.097295

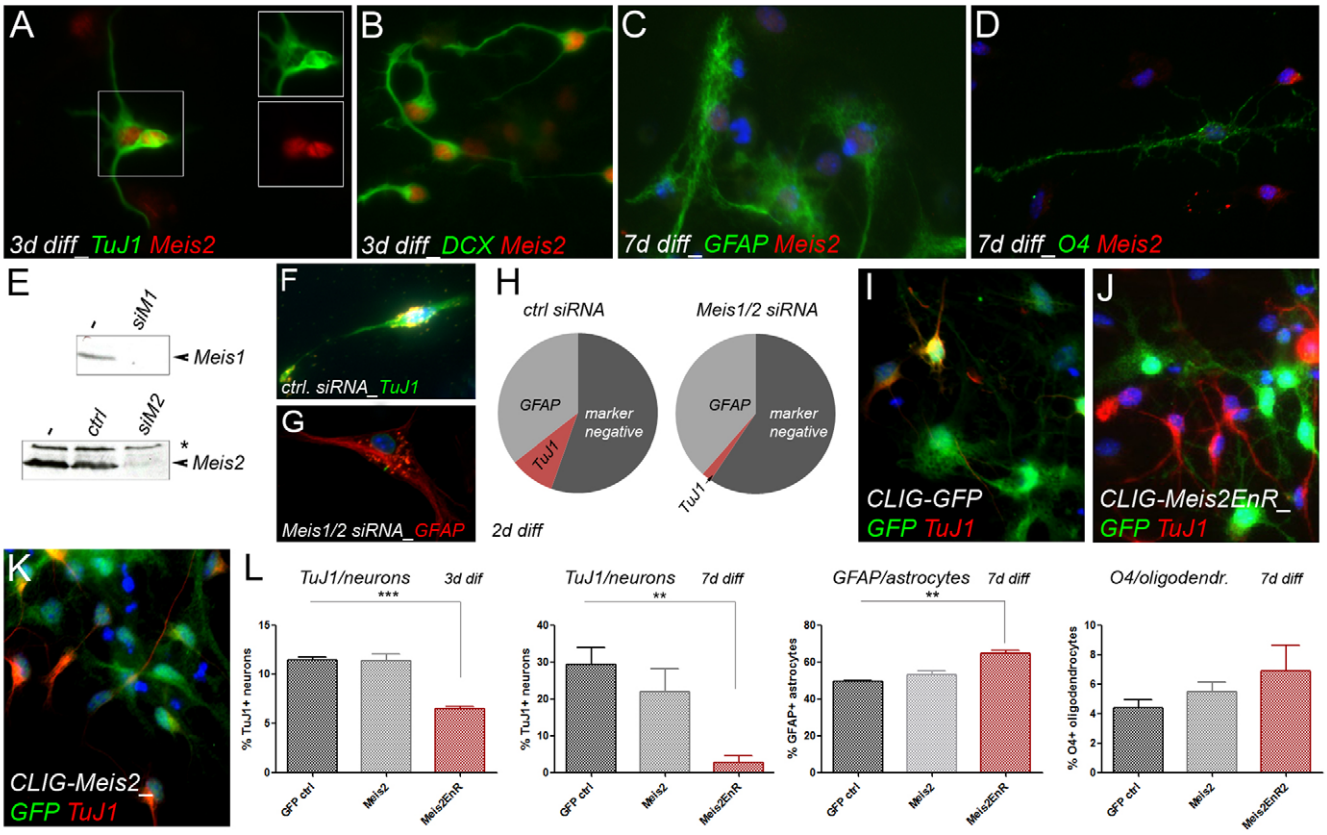

Fig. 3. Neuronal differentiation of neurosphere-derived cells requires Meis2 *in vitro*. (A,B) Co-labeling for Meis2 (red) and neuroblast markers (green) 3 days after growth factor withdrawal: (A) TuJ1; (B) Dcx. (C,D) Meis2 (red) and glial marker proteins (green) 7 days after growth factor withdrawal: (C) Gfap; (D) O4. (E) Western blot analysis of Meis1 (upper panel) and Meis2 (lower panel) expression after transfection with the siRNAs indicated. –, non-transfected; ctrl, scrambled control RNA; siM1, *Meis1*-specific siRNA; siM2, *Meis2*-specific siRNA; asterisk marks an unspecific band recognized by the Meis2 antibody, which is not sensitive to Meis2 knockdown (and does not interact with Pax6; Fig. 6B). (F,G) Representative examples of cells transfected with the control siRNA (F) or *Meis1/2* siRNA (G). (H) Quantification of the results showing the proportion of cells expressing Gfap, TuJ1 or no marker. (I-K) TuJ1 (red) and GFP (green) in differentiated neurospheres, which were infected with the retroviruses indicated: (I) CLIG-GFP control; (J) CLIG-Meis2EnR; (K) CLIG-Meis2. (L) Quantification of the results. Error bars indicate s.e.m. ***P*<0.01; ****P*<0.001. Cell nuclei are counterstained with DAPI in C,D,F,G,I-K.

treated cultures typically contained fewer fluorescent siRNA speckles than did astroglia or undifferentiated cells, indicating that they may have escaped efficient Meis knockdown (supplementary material Fig. S2). To substantiate these observations, we infected growing neurospheres with bicistronic retroviruses carrying GFP either alone or together with Meis2 or with a chimeric fusion protein in which the coding sequence of Meis2 was linked to the *Engrailed* repressor domain (Meis2EnR; Fig. 3I-L; supplementary material Fig. S3). In previous studies investigating Meis2 in the context of retinal, tectal or lens development, we and others had shown that MeisEnR fusion proteins function as dominant negatives exclusively in cells that endogenously express Meis1 or Meis2 (Agoston and Schulte, 2009; Heine et al., 2008; Zhang et al., 2002). Neurosphere cells that were transduced with Meis2EnR and then allowed to differentiate for three days generated markedly fewer TuJ1-expressing neurons than did non-transfected cells or cells that were infected with the GFP-bearing control virus (Fig. 3I,J,L; data not shown). To examine whether Meis2EnR inhibited neuronal differentiation or merely delayed it, we differentiated Meis2EnR-transduced neurosphere cells for 7 days. Still, TuJ1-positive neurons were very infrequent in the cultures, suggesting that Meis2EnR indeed interfered with neurogenesis (Fig. 3L). Concomitantly, the percentage of Gfap-positive astrocytes generated from Meis2EnR-infected cells increased (Fig. 3L). Meis2EnR-transduced neurosphere cultures also contained more oligodendrocytes than did GFP-transduced controls, although their numbers did not reach statistical significance, possibly as a result of the relative low frequency at which these cells differentiate *in vitro* and their protracted maturation (Fig. 3L). Forced expression of Meis2 did not affect neurogenesis or gliogenesis to a statistically significant degree relative to the GFP control (Fig. 3K,L).

To relate the observations described above to cell fate decisions *in vivo*, we stereotactically injected these retroviruses into the SVZ of adult mice. Three days after injection of the GFP-bearing control virus, many infected cells had entered the RMS and migrated towards the OB, and 92.1% (±2.44% s.e.m.) of them already expressed neuronal markers such as PSA-NCAM (Fig. 4A,D). Upon transduction of Meis2, still 78.9% (±7.4% s.e.m.) of the transduced cells were immunoreactive for PSA-NCAM (Fig. 4B,D), whereas only 8.5% (±1.0% s.e.m.) of the Meis2EnR transduced cells expressed PSA-NCAM (Fig. 4C,D). Comparable results were obtained for Dcx expression (Fig. 4E-G). Notably, the proportion of Gfap-positive astroglia generated from transduced cells at 4 days post transduction increased from 0.58% (±0.293% s.e.m.) in GFP-injected controls to 9.8% (±4.4% s.e.m.) in Meis2EnR-injected animals (Fig. 4H-J). Likewise, 10 days post injection retrovirally labeled neuroblasts were still streaming from the SVZ in GFP- but not in Meis2EnR-transduced animals (data not shown). Interestingly,

Development (2014) doi:10.1242/dev.097295

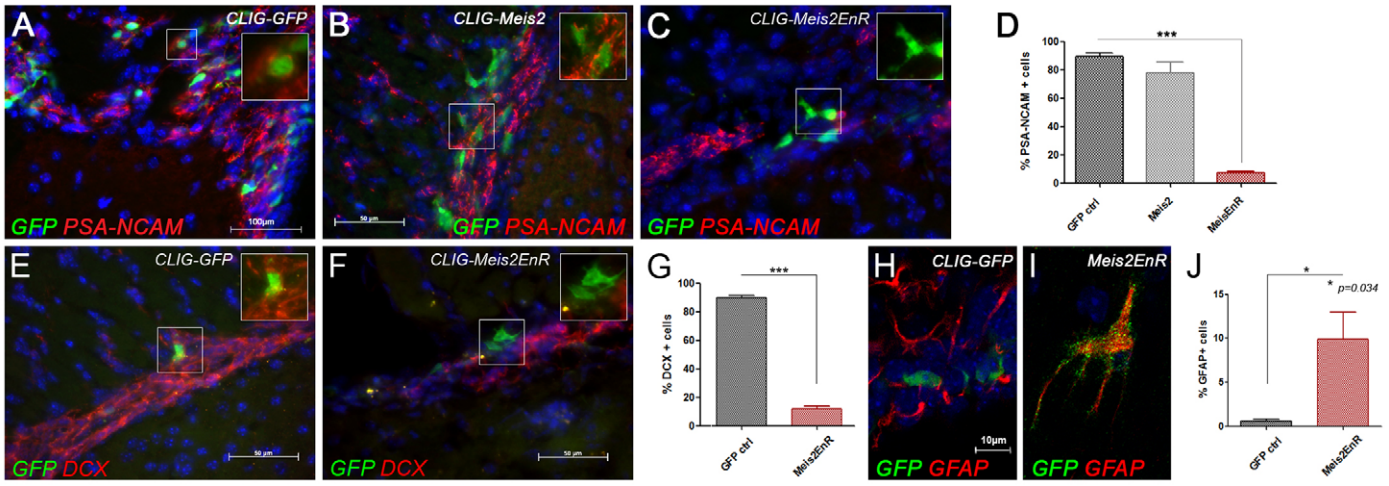

Fig. 4. Meis2EnR transduction blocks neurogenesis *in vivo*. (A-C) PSA-NCAM (red) and GFP (green) in the RMS, three days after injection of the respective retroviruses into the SVZ: (A) CLIG-GFP; (B) CLIG-Meis2; (C) CLIG-Meis2EnR. (D) Quantification of the results. (E-G) Dcx (red) and GFP (green) in the RMS, three days after retroviral injection into the SVZ: (E) CLIG-GFP; (F) CLIG-Meis2EnR; (G) quantification of the results. (H,I) Gfap (red) and GFP (green) in the SVZ, four days after transduction of CLIG-GFP (H) or CLIG-Meis2EnR (I) into the SVZ. (J) Quantification of the results. Error bars indicate s.e.m. **P*<0.05; ****P*<0.001. Cell nuclei in A-I are counterstained with DAPI. Scale bars: 50 µm; 10 µm in H.

at all time points analyzed retrovirally transduced cells were clearly less frequent in Meis2EnR-infected specimen than in GFP transduced controls, despite the fact that equal titer viruses were injected and no increased cell death was observed (data not shown). This observation corresponds well with a very recent report in which continuous live imaging of SVZ-derived progenitor cells revealed that neurogenic cells undergo considerably more rounds of cell division before they terminally differentiate than do progenitors fated to become astroglia (Ortega et al., 2013). We therefore concluded that Meis2 is necessary for neuronal differentiation of SVZ-derived progenitor cells and that interfering with its function favors astrogliogenesis over neurogenesis.

Meis activity is required for dopaminergic periglomerular fate specification *in vivo*

The near-ubiquitous Meis2 expression in dopaminergic PGNs and its colocalization with Pax6 prompted us to investigate a possible role of Meis2 in the specification of this neuronal subtype. In order to target this population, we injected the CLIG-retroviruses into the RMS (Hack et al., 2005; Mendoza-Torreblanca et al., 2008). Three weeks after injection of the GFP-expressing control virus, nearly half of the GFP-positive PGNs expressed Pax6 (45.25±2.25% s.e.m.), and 6.7% (±0.9% s.e.m.) were already labeled for Th (Fig. 5A,D), increasing to 32.1% (±1.97% s.e.m.) at 60 days post injection, consistent with the protracted differentiation of dopaminergic PGNs (Fig. 5D). Dopaminergic PGNs were also readily generated from Meis2-transduced neuroblasts (Fig. 5B,D). By contrast, Meis2EnR-transduced cells populating the GL exhibited the cellular morphology of mature neurons, but none of them expressed Pax6 or Th (Fig. 5C,D; supplementary material Fig. S4) and only a few Meis2EnR-transduced cells were immunoreactive for Gad67 (data not shown). Consistent with their morphology, Meis2EnR-expressing cells did not revert to a neuroblast fate, as evident in the absence of TuJ1 or PSA-NCAM expression (data not shown). The absence of GAD- or Th-expression is thus unlikely to result from compromised differentiation. Notably, the proportion of calretinin-immunoreactive PGNs increased following Meis2EnR transduction, indicative of a change in cell fate from dopaminergic to calretinin+ PGNs (supplementary material Fig. S4). Generation of calbindin+ cells, by contrast, was unaffected by Meis2EnR misexpression (5.9±1.2% for Meis2EnR, 5.2±1% for GFP control). These results are consistent with a previous study, which showed that loss of Pax6 or forced expression of a function-blocking form of Dlx2 reduced the proportion of dopaminergic neurons and increased the number of calretinin+ cells without affecting the calbindin+ PGN population (Brill et al., 2008). Conversely, Dlx2 overexpression was shown to increase the proportion of Th^+ PGNs at the expense of calretinin+ PGNs (Brill et al., 2008).

Meis2 forms heteromeric complexes with Pax6 and Dlx2 in the adult SVZ-OB system

Meis family proteins frequently function as co-factors of other transcriptional regulators (Moens and Selleri, 2006) and forced

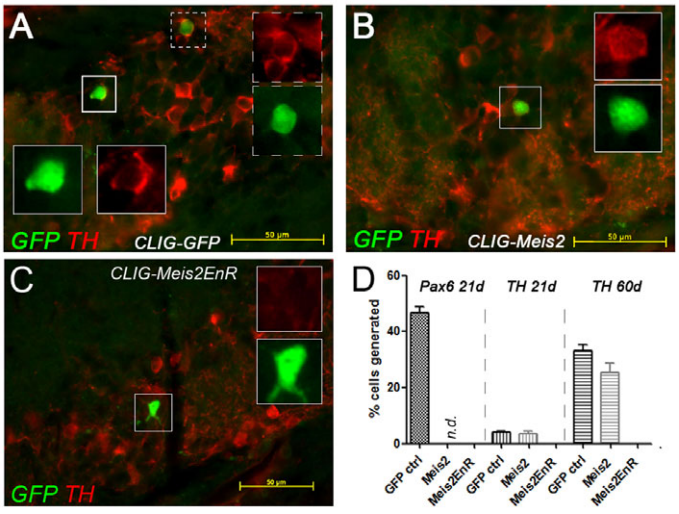

Fig. 5. Meis2EnR transduction blocks dopaminergic fate specification *in vivo*. (A-C) Cross sections through the GL of mice stained for GFP (green) together with Th (red), 21 days after virus injection into the RMS: (A) CLIG-GFP; (B) CLIG-Meis2; (C) CLIG-Meis2EnR. (D) Quantification of the results. Error bars indicate s.e.m. Meis2EnR transduced cells in the GL did not express Pax6 or Th at 21 or 60 days after virus injection. n.d., not done.

Development (2014) doi:10.1242/dev.097295

expression of Meis2 was not sufficient to induce neuronal differentiation or dopaminergic fate specification in our system. This suggests that Meis2 may synergize with other transcription factors to exert its function in adult SVZ neurogenesis and PGN specification. On the basis of their expression patterns, Pax6 and Dlx2 are excellent candidates: both proteins dimerize in the SVZ and OB, they function cooperatively in SVZ neurogenesis and dopaminergic PGN specification and their expression colocalizes with that of Meis2 in the RMS and OB (Brill et al., 2008; Hack et al., 2005; Kohwi et al., 2005; Kohwi et al., 2007).

Pull-down experiments with a GST-tagged form of Meis2 and protein extracts from OB or SVZ tissue enriched two Pax6-immunoreactive protein bands of 48 and 51 kDa, presumably corresponding to canonical Pax6 and the alternatively spliced Pax6(5a) (ppt; Fig. 6A, upper panel). Upon re-probing the blots with the panDlx antibody, prominent Dlx-specific protein bands of 38 kDa and 32 kDa (presumably corresponding to Dlx2 and Dlx1, respectively) were detected in the Meis2 precipitates (Fig. 6A, lower panel). Presence of Meis2- and Pax6-containing protein complexes *in vivo* was corroborated by co-immunoprecipitation experiments from nuclear extracts of OB tissue (Fig. 6B). Because co-expression of Meis2 and Pax6 in the OB is restricted to migrating neuroblasts and dopaminergic PGNs, only a fraction of the Meis2 protein present in the lysates was found to associate with Pax6. Meis2-Pax6 interaction was direct, occurred *in vitro* with the three major Pax6 isoforms that are expressed in the brain, canonical Pax6 [Pax6(−5a)], the longer Pax6(+5a) isoform, and the truncated paired-less Pax6 variant, and involved the Meis2 homeodomain (Fig. 6C-F). In addition, mutual direct interaction between Pax6, Dlx2 and Meis2 was observed *in vitro* (Fig. 6G,H). Collectively, these results argue that Meis2 partakes in Pax6-Dlx2-containing transcription factor complexes in the SVZ/OB neurogenic system.

Meis2, Dlx2 and Pax6 are also co-expressed in other regions of the embryonic and adult central nervous system, including the neural retina (Bumsted-O'Brien et al., 2007; de Melo et al., 2003). Indeed, Meis2-Pax6- and Meis2-Dlx-containing protein complexes were successfully purified from retinal extracts by pull-down and immunoprecipitation (supplementary material Fig. S5). Meis2-Pax6-Dlx2-containing transcriptional complexes are thus part of an evolutionarily conserved program.

Meis2 and Pax6 functionally interact

To test whether Meis2, Pax6 and Dlx2 functionally cooperate during adult SVZ neurogenesis, we took advantage of the pro-neurogenic activity of Pax6 (Hack et al., 2005). Neurosphere cells were transfected with an siRNA cocktail targeting *Meis1* and *Meis2*, immediately infected with Pax6-expressing retroviruses and differentiated 24 hours later. Upon retroviral transduction of Pax6, SVZ-derived neurospheres generated neurons at high frequency (Fig. 6I). By contrast, when Pax6 gain of function was combined

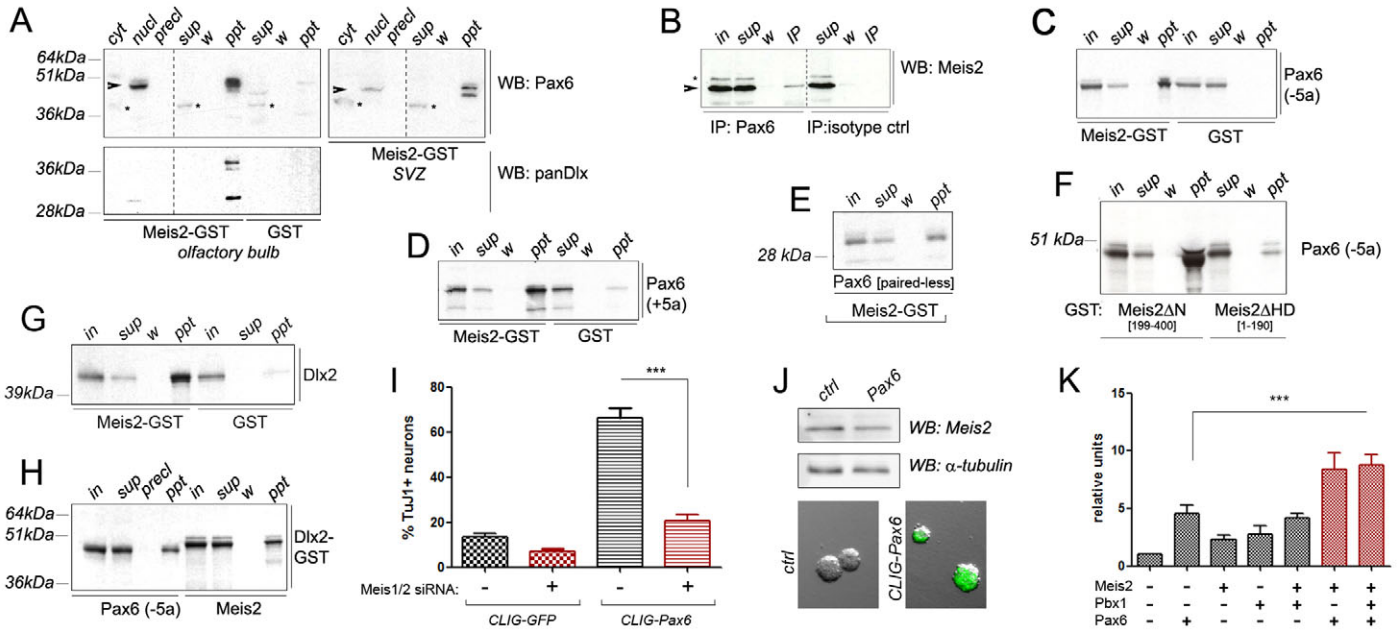

Fig. 6. Direct interaction and functional cooperation of Meis2 with Pax6. (A) GST pull-down from protein extracts prepared from the OB (left) or SVZ (right). Top panels: western blot analysis (WB) with an antibody against Pax6. Protein bands corresponding to known Pax6 isoforms are indicated by arrowheads, asterisks mark putative unspecific bands. Bottom panel: western blot analysis with a Dlx-specific antibody on the same blot as above. Dlx-specific signals could not be detected from SVZ extracts, presumably because the Dlx-protein concentration in these cells is too low. (B) Immunoprecipitation with antibodies against Pax6 (left) or an isotype-specific control (right) probed for Meis2; the asterisk indicates an unspecific band. (C-E) GST pull-down experiments with radiolabeled proteins produced *in vitro*: Pax6(−5a) (C), Pax6(+5a) (D) and paired-less Pax6 (E) bind to Meis2-GST but not to GST alone. (F) Pax6(−5a) strongly binds to an N-terminally deleted Meis2 lacking the MEINOX domain (Meis2ΔN), but only weakly to Meis2 lacking the homeodomain (Meis2ΔHD). (G) Recombinant, ^{35}S-labeled Dlx2 binds directly to Meis2-GST. (H) Dlx2-GST associates with radiolabeled Pax6(−5a) and Meis2. (I) Simultaneous Meis2 knockdown and Pax6 transduction in SVZ-derived neurospheres; histogram showing the percentage of neurons generated from progenitor cells transduced with GFP or GFP+Pax6 in the presence or absence of *Meis1/2*-specific siRNAs. (J) Meis2 protein expression in neurosphere cells transduced with Pax6 relative to non-transfected controls (upper panel); WB for α-tubulin as loading control (lower panel). (K) Activation of the DCX2073 enhancer/promoter construct by Meis2, Pbx1 and Pax6 as indicated. Reporter activation is expressed as fold induction relative to reporter activity in the absence of Meis2, Pbx1 and Pax6. cyt, cytoplasmic extract; in, input; IP, immunoprecipitate; nucl, nuclear extract; ppt, precipitate of the pull-down reaction; precl, protein precipitates pre-cleared with glutathione-coupled beads prior to the addition of the GST-fusion protein; sup, supernatant of the pull-down or IP reaction; w, final wash. Error bars represent s.e.m. ***P<0.001.

Development (2014) doi:10.1242/dev.097295

with *Meis1/2* knockdown, the neurogenic potential of Pax6 was largely abolished (Fig. 6I). However, the number of neurons produced from Pax6- *siMeis1/2* double-transfected cells still slightly exceeded basal levels. This may result from uneven uptake of the siRNAs across the neurosphere cultures leading to some cells having escaped *Meis1/2* knockdown. The loss of Pax6-derived neurogenic activity in the absence of Meis1/2 could be explained by three different scenarios: (1) Pax6 acts upstream of Meis2 and regulates neurogenesis by controlling Meis2 expression, (2) Pax6 and Meis2 function in parallel, non-redundant pathways and regulate different sets of target genes necessary for neuron differentiation, or (3) complex formation with Meis2 is essential for the neurogenic activity of Pax6. To test whether *Meis2* is a Pax6 target gene during SVZ neurogenesis, we transduced neurosphere cultures with Pax6. Meis2 protein is weakly expressed in neurosphere cells, but levels were not raised by forced Pax6 expression (Fig. 6J). To test the possibility that Meis2 and Pax6 regulate common target genes, we focused on Dcx, a microtubule-associated protein, expression of which is characteristic of newborn, migrating neurons, including neuroblasts of the RMS (Francis et al., 1999; Gleeson et al., 1999). *In silico* analysis of known genomic regions that act as Dcx enhancers or promoters revealed the presence of stretches of overlapping or adjacent consensus sites for Pax6, Dlx and Meis/Pbx (Karl et al., 2005; Piens et al., 2010) (supplementary material Fig. S6). Indeed, a luciferase reporter in which firefly luciferase expression is driven by a 2073-bp genomic fragment of the murine *Dcx* locus (DCX 2073) was readily activated in HEK293T cells by co-transfection of Pax6, of Meis2, of the Meis-interacting protein Pbx1 or of Meis2 together with Pbx1 (Fig. 6K). This corresponds well to previous studies, which had shown that Meis2 possesses transcriptional activator function (Heine et al., 2008; Hyman-Walsh et al., 2010). Importantly, transfection of Meis2 together with Pax6 (with or without Pbx1) significantly increased reporter activation over transfection of each transcription factor alone, arguing against the possibility that Meis2 and Pax6 regulate neurogenesis through separate pathways and by means of different target genes. Collectively, our results argue that Pax6 requires Meis2 to promote neurogenesis from SVZ derived stem and progenitor cells.

To investigate whether Meis2 and Pax6 act directly on *Dcx in vivo*, we performed chromatin immunoprecipitation (ChIP) from adult SVZ-derived neurospheres that had been differentiated *in vitro* towards the neuronal lineage. We focused on two stretches of closely located binding sites for Meis2, Pax6 and Dlx, termed DCXI and DCXII (Fig. 7A; supplementary material Fig. S6). The Meis2 antibody efficiently precipitated both *Dcx* chromatin fragments, as did an antibody specific for Pax6 and the panDlx antibody (Fig. 7B,C). In young neurons, the *Dcx* promoter region is thus bound by Meis2, Pax6 and Dlx at closely located sites. An unrelated genomic region, the promoter/enhancer of *Gapdh*, was not enriched (Fig. 7C). As expected for young neurons, RNA polymerase II (RNApolII) also occupied the *Dcx* and *Gapdh* promoter regions. ChIP with the Meis2-specific antibody from undifferentiated SVZ-derived neurosphere cultures, by contrast, did not enrich the DCXI or DCXII chromatin fragments above background levels (Fig. 7D; data not shown). Thus, the *Dcx* locus is not bound by Meis2 prior to cellular differentiation. Specificity of the Meis2 antibody was demonstrated by two independent approaches. First, Dcx was not precipitated from acutely dissociated dentate gyrus (where Meis2 protein is absent but Dcx is strongly expressed) (Fig. 7D). Second, the Meis2 antibody did not precipitate the myogenin promoter, which is bound by Meis2 in differentiating myoblasts (Berkes et al., 2004) from neurons (data not shown). To relate Meis2 occupancy to *Dcx* enhancer/promoter activation, we generated truncated Dcx reporters, which lack the TALE/Pax6-binding sites DCXI and/or DCXII. As observed for the DCX2073 enhancer/promoter, reporter activity of a shorter Dcx enhancer construct (DCX1112) was

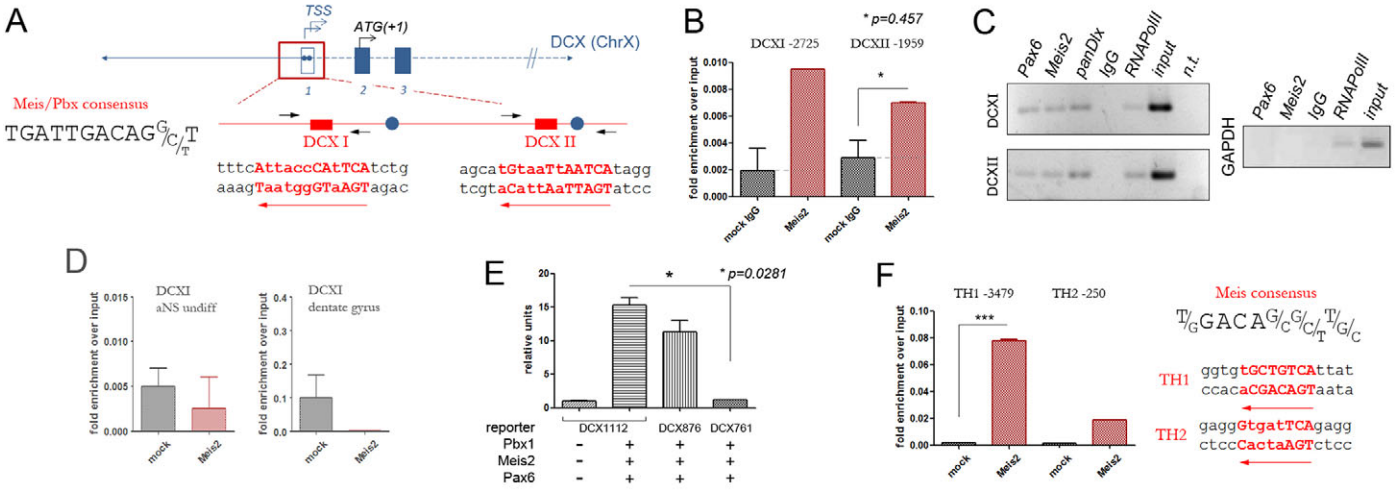

Fig. 7. *Dcx* and *Th* promoter regions are occupied by Meis2 *in vivo*. (A) Schematic of the mouse *Dcx* regulatory region analyzed (red box) relative to the *Dcx* genomic locus; filled boxes indicate coding exons; exons 1-3 are numbered; blue dots mark putative transcriptional start sites (TSS); the relative location and sequence of the two Meis2 binding sites (DCXI and DCXII) are shown and the published consensus binding sequence for Meis/Pbx is given for comparison (Chang et al., 1997). (B,C) ChIP on chromatin from *in vitro* differentiated neurosphere cultures enriched for neurons. (B) ChIP-qPCR for Meis2 or an unspecific IgG cocktail on the DCXI and DCXII sites, fold enrichment over input is plotted. (C) ChIP for DCXI, DCXII and Gapdh with the antibodies indicated; PCR products during the logarithmic accumulation of amplicons are visualized on agarose gels. (D) ChIP-qPCR for Meis2 or an unspecific IgG cocktail on chromatin from undifferentiated SVZ-derived neurospheres (left) or on chromatin from acutely dissected dentate gyrus (right). (E) Luciferase reporter assays of a shorter *Dcx* promoter/enhancer construct containing the TALE/Pax6-binding sites DCXI and DCXII (DCX1112), lacking binding site DCXI (DCX876) or lacking both sites (DCX761) upon stimulation by Meis2, Pbx1 and Pax6. Reporter activation is expressed as fold induction relative to the activity of DCX1112 in the absence of Meis2, Pbx1 and Pax6. (F) ChIP-qPCR for Meis2 or unspecific IgGs on the *Th* promoter/enhancer; sequences of the Meis2-bound binding sites and the Meis consensus binding motif are given for comparison. mock IgG, unspecific control; n.t., no template. Error bars represent s.e.m. **P*<0.05; ****P*<0.001.

Development (2014) doi:10.1242/dev.097295

strongly stimulated by co-transfection of Meis2, Pbx1 and Pax6 (Fig. 7E). Deletion of the DCXI binding site resulted in a modest reduction of reporter activity upon co-transfection with the three transcription factors, whereas deletion of both DCXI and DCXII completely abolished transactivation by Meis2/Pbx1/Pax6 (Fig. 7E). Hence, Meis2 directly transactivates *Dcx* and its association with *Dcx* regulatory elements accompanies neuronal differentiation specifically in adult SVZ-derived neurons.

Because Meis2 function was also required for dopaminergic neuron differentiation *in vivo*, we also considered Th, the rate-limiting enzyme for the production of L-DOPA, as possible Meis2 target. *In silico* analysis of a published promoter/enhancer region of the *Th* gene (NCBI Acc. No. AF415235) revealed several Meis consensus binding sites. *In vivo* ChIP analysis with the Meis2-specific antibody and chromatin prepared from the adult mouse OB profoundly enriched a consensus binding motif located at position −3479 relative to the *Th* start codon and to a lesser extent a motif located at position −250 (Fig. 7F). Meis2 thus functions in adult SVZ neurogenesis and PGN specification by directly acting on the regulatory regions of genes that are important in both contexts: *Dcx* for differentiation towards a general neuronal fate and *Th* for dopaminergic neurotransmitter subtype specification.

DISCUSSION

Here, we present evidence implicating the TALE homeodomain protein Meis2 in two key aspects of adult olfactory bulb neurogenesis in mammals. Targeted manipulations with retroviral vectors expressing function-blocking forms or with siRNAs demonstrated that Meis activity in the SVZ is cell-autonomously required for neuronal differentiation, and Meis2 activity in the RMS is important for the generation of dopaminergic PGNs in the OB. Meis2 forms higher order protein complexes and functionally cooperates with Pax6, a known regulator of SVZ neurogenesis and dopaminergic PGN specification. In addition, we identify *Dcx* and tyrosine hydroxylase as direct Meis2 target genes. Together, these findings contribute to an emerging model of how the concerted activities of transcriptional regulators steer cell fate decisions in the adult SVZ-OB system.

Multi-protein networks involving Meis family members in the brain

Meis family proteins form dimeric or trimeric complexes with other transcription factors. In the hindbrain, the PBC proteins Pbx1-4 and members of the Hox clusters are major Meis-binding partners (Elkouby et al., 2012; Maeda et al., 2002; Vlachakis et al., 2001; Wassef et al., 2008), but only a few proteins are known to associate with Meis family proteins in the mes-, di- or telencephalon. These include Oct1 (Slc22a1), which cooperates with the Meis-related Prep1 (Pknox1) to control expression of gonadotropin-releasing hormone in the hypothalamus, and Otx2, Pax3 and Pax7 during tectal development (Agoston and Schulte, 2009; Agoston et al., 2012; Rave-Harel et al., 2004). The findings reported here now identify Pax6 and Dlx2 as Meis-interacting proteins in the forebrain. Pax6, an evolutionarily highly conserved transcription factor, controls proliferation, patterning, and cell fate specification in the brain and retina. Different variants of Pax6 exist, which contact DNA through distinct domains. Canonical Pax6[Pax6(−5a)] binds DNA primarily through the N-terminal portion of the paired domain (the PAI-domain), in Pax6(+5a) the DNA-binding potential of the C-terminal RED-domain predominates, whereas the ‘paired-less’ isoform utilizes the homeodomain for DNA binding (Epstein et al., 1994; Kleinjan et al., 2004; Kozmik et al., 1997; Mishra et al., 2002). All three isoforms recognize distinct DNA consensus sites and participate in the regulation of different developmental processes (Epstein et al., 1994; Haubst et al., 2004; Singh et al., 2002; Walcher et al., 2013). As we show here, all three isoforms can directly associate with Meis2. Combining Pax6 gain of function with Meis1/2 knockdown *in vitro* demonstrated that the neurogenic potential of Pax6 requires Meis protein activity, which underscores the importance of Meis-Pax6 complex formation in the SVZ/OB system. Notably, Pax6 and Dlx2 also bind to Meis2 in protein extracts of the embryonic chick eye. This observation not only suggests that Meis2 may function as a more general Pax6- and Dlx2-binding partner, but also argues for the evolutionary conservation of a Meis-Pax-Dlx-containing molecular cassette. Recruitment of genetic components, which have been adapted to new physiological contexts, is not unprecedented. For instance, vertebrate muscle development requires the synergistic activities of homologs of the *dachshund*, *eyes absent* and *sine oculis* gene products, which act together to control eye development in *Drosophila melanogaster* (Heanue et al., 1999). It remains to be determined, however, whether Meis2, Pax6 and Dlx2 act as a trimeric protein complex or as individual Meis-Pax, Meis-Dlx and Pax-Dlx dimers and whether other proteins can also associate with them. It is also interesting to note that *Pax6* is a Meis target gene in the retina, lens and pancreas (Carbe et al., 2012; Heine et al., 2008; Zhang et al., 2002; Zhang et al., 2006). Conversely, Pax6 was recently reported to bind to upstream regulatory regions of the *meis1* gene in the embryonic zebrafish retina (Royo et al., 2012). The possibility of mutual regulation between Meis and Pax6 is intriguing and may represent a simple but effective way by which cell fate decisions can be stabilized. Whether Pax6 expression is also under direct control of Meis in the adult SVZ, RMS and OB is unknown, as the regulatory elements that drive Pax6 expression in these cells and tissues have, to our knowledge, not yet been characterized.

Meis2 participates in adult neurogenesis and PGN subtype specification

siRNA-mediated knockdown or retroviral misexpression of function-blocking constructs of Meis2 inhibited general neurogenesis when SVZ-derived stem and progenitor cells were transduced and dopaminergic PGN differentiation when neuroblasts in the RMS were targeted. Meis2 thus participates in the transcriptional regulation of genes involved in both processes. Indeed, Meis2 is bound to promoter regions of the *Dcx* and *Th* genes in SVZ-derived young neurons and the OB, respectively. Interestingly, Dcx expression depends on the SoxC type transcription factors Sox4 and Sox11 in newly generated hippocampal neurons (Mu et al., 2012). Because Meis2 (and the related Meis1) are not expressed in the hippocampus, context-dependent differences probably exist in the regulation of basic neurogenic programs, such as the transcriptional activation of *Dcx*, in both neurogenic niches.

In contrast to Pax6, Dlx2 or Sox4/11, Meis2 transduction alone did not promote neurogenesis. This is surprising at first, considering that it forms higher order protein complexes with Pax6 and Dlx2. Possible explanations derive from studies on skeletal muscle differentiation and mid- and hindbrain development. MyoD, a bHLH transcription factor required for the initiation of skeletal muscle differentiation, is targeted to promoters of downstream genes, such as myogenin, by a Pbx/Meis-containing protein complex that is present at these sites prior to MyoD (Berkes et al., 2004). In the embryonic zebrafish hindbrain, by contrast, Meis3 displaces histone deacetylase 1 (Hdac1) from Hox/Pbx-containing

Development (2014) doi:10.1242/dev.097295

transcriptional complexes and thereby overrides Hdac-mediated repression of Hox target genes (Choe et al., 2009). Similarly, Meis2 can release Otx2 from groucho-mediated repression during early stages of chick midbrain development, which entails the expression of tectum-specific genes (Agoston and Schulte, 2009). In all three systems, Meis family members activate transcription indirectly by orchestrating the temporally and spatially controlled assembly and disassembly of transcription factor complexes, which build around tissue-specific master regulatory proteins. The results reported here raise the intriguing possibility that Meis proteins may fulfill a similar function during the activation of neurogenic programs in the adult SVZ-OB system. In contrast to the systems described above, however, the interplay of transcriptional regulators involved in adult SVZ-OB neurogenesis, the hierarchy in which they act and the regulatory elements to which they bind are still largely unknown. A more comprehensive view of the transcription factors that orchestrate adult SVZ neurogenesis, and the regulatory elements they act upon is therefore required before the precise role of Meis proteins in this context can be determined.

MATERIALS AND METHODS

Animals and stereotactic injections

Stereotactic injections in 5- to 8-week-old C57/bl6J mice were performed as described (Brill et al., 2008). All procedures involving animals were approved by the local animal care committee and were in accordance with the law for animal experiments issued by the state government. Neurospheres were prepared, propagated and differentiated as described (Brill et al., 2008). Second or third passage neurosphere cells were used for all experiments but ChIP, for which first-passage neurospheres were used. For retroviral infection, neurospheres were resuspended in 1.2 ml EGF/FGF2-containing medium and incubated for 3 hours at 37°C in the presence of retroviral stocks at 2-4×10^4 CFU/ml. The average rate of neurosphere transduction was 64.77% (±23.02%; n=17 independent experiments).

Analysis of Meis2-containing protein complexes

GST pulldown and co-immunoprecipitation experiments were performed as detailed (Agoston and Schulte, 2009). Meis2, Dlx2 and Pax6 were generated *in vitro* by TNT-coupled transcription/translation (Promega) according to the manufacturer's instructions. Truncated forms of the proteins have been described previously (Agoston et al., 2012) or were generous gifts from D. Engelkamp (University Erlangen-Nürnberg, Germany)

Reporter assay

The luciferase reporter construct DCX2073 contains the genomic fragment of NT –3838 to NT –1765 upstream of the DCX start codon [corresponding to pdcx2kb of Piens et al. (Piens et al., 2010)] subcloned into pGL3basic (Promega). Additional luciferase reporter constructs contain (relative to ATG): DCX1112: NT –2877 to –1765 [overlapping region of the promoter/enhancer regions identified previously (Piens et al., 2010 and Karl et al., 2005)]; DCX876: NT –2641 to –1765 (deleting the ChIP amplicon surrounding TALE binding site DCXI); DCX761: NT–2641 to –1880 (deleting TALE bindings sites DCXI and DCXII). HEK293T cells were chosen for reporter assays because of their low endogenous Meis2 expression. Cells were transfected with 140 ng of the above reporter constructs together with 40 fmol each of Pbx1b-pCS2+, Meis2b-pMIWIII and Pax6(–5a)-pMIWIII. A plasmid expressing *Renilla* luciferase under the control of the human elongation factor 1 (Hef-1) promoter was co-transfected for normalization, luciferase assays were performed in triplicates 48 hours after transfection according to Dyer et al. (Dyer et al., 2000).

In situ hybridization, immunohistochemical analysis and BrdU labeling

The cDNAs used to generate *in situ* probes were as described (Heine et al., 2008) or were generous gifts from D. Engelkamp (University Erlangen-Nürnberg, Germany). *In situ* hybridization on 70-µm vibratome sections of paraformaldehyde (PFA)-fixed tissue was performed as described (Heine et al., 2008), immunohistochemical detection on 13-µm frozen sections as detailed (Bumsted-O'Brien et al., 2007), and immunohistochemical detection on 50- to 70-µm vibratome sections as described (Brill et al., 2008). Primary antibodies used are listed in supplementary material Table S1. Unless noted in the text, the absolute cell numbers that were counted for each condition and the number of technical replicates are given in supplementary material Tables S3-S5. Neurogenin 2-expressing cells were visualized in a published transgenic mouse line (Berger et al., 2004). For detection of proliferating cells, the DNA base analogon 5′-bromo-2′-deoxyuridine (BrdU; Sigma Immunochemicals) was injected intraperitoneally (50 mg/kg of body weight) 1 hour before perfusion to label fast-proliferating cells. For long-term labeling, BrdU was added for three weeks to the drinking water at a concentration of 1 mg/ml and exchanged twice a week.

Retroviral constructs, virus preparation and siRNA-mediated knockdown

Meis2EnR blocks the function of endogenous Meis1 and Meis2 in a dominant-negative manner and the effect of Meis2EnR is specific for tissues expressing endogenous Meis proteins (Agoston and Schulte, 2009; Heine et al., 2008). To generate CLIG-Meis2, full-length murine Meis2b was amplified from mouse SVZ tissue and cloned into pCLIG (Hojo et al., 2000). CLIG-GFP served as control. Viral stocks were prepared as described (Brill et al., 2008) and diluted to equal titers before injection.

Oligonucleotide sequences for siRNA-mediated knockdown of Meis1 or Meis2 expression were 5′-CAGUGAAGAUGUAACAAGA-3′ for murine Meis1 and 5′-UCAUGAUAUUUGUCGCGAC-3′ for murine Meis2 (Cy5-labeled at 5′ ends; Eurogentech, Liège, Belgium). RNA duplexes were transfected into neurospheres using GeneTrans II (MoBiTec, Germany; following manufacturer's instructions). Knockdown was at least 80% judged by western blot; control siRNAs were ineffective. Twenty-four hours after viral or siRNA transfection, the cells were differentiated as described (Brill et al., 2008).

Chromatin immunoprecipitation (ChIP)

First passage neurosphere cells (1-2×10^7 per ChIP) were transduced with Pax6 for 48 hours, plated on laminin-coated tissue culture dishes at a density of 5×10^6 cells per 10-cm dish and differentiated for 7 days in the presence of 2 ng/ml FGF2 and 20 ng/ml BDNF (Preprotec). Per ChIP experiment and antibody used, 1×10^7 *in vitro*-differentiated cells or undifferentiated neurosphere cells, 3.5 freshly dissected dentate gyri or 0.7 OB were used. ChIP was performed according to Kutejova et al. (Kutejova et al., 2008) with the following modifications: chromatin was cross-linked in 2% freshly prepared PFA for 23 minutes at 4°C under gentle agitation. OB or dentate gyrus cells were mechanically dissociated on ice, washed twice with PBS (containing Complete tablets; Roche) and cross-linked as above. Chromatin was sheared to an average length of 200-600 bp with a Bioruptor Plus (Diagenode, Liège, Belgium). Ten micrograms of the antibodies listed in supplementary material Table S1 were used for chromatin precipitation, except RNA polymerase II for which 2 µg were used. Immunoprecipitation was carried out over night at 4°C. Chromatin-immune complexes were isolated with a 1:1 mixture of ProteinA:ProteinG Dynabeads (Invitrogen). Crosslinking was reversed for 5 hours at 65°C with shaking (at 1500 rpm). DNA was purified from the precipitates with the MinElute PCR Purification Kit (Qiagen; final elution volume 50 µl). Chromatin immunoprecipitates were amplified with the primers listed in supplementary material Table S2. For quantitative real-time PCR, 8 µl of the eluted chromatin samples were used per reaction. PCR was performed in duplicate with the ABsolute QPCR SYBR Green Fluorescein Mix (ThermoFisher Scientific) on a BioRad MyiQ Real-Time PCR Detection System (Bio-Rad Laboratories). Enrichment of precipitated DNA was determined relative to the input (1:100) as $100\times2^{(Ct\ adjusted\ Input\ -\ Ct\ IP)}$. Standard error was calculated between experimental replicates. For regular PCR, the logarithmic phase of amplification was determined empirically based on the amplification of the precipitates obtained with RNA polymerase II-specific antibodies and the mock-IgG controls. Generally, 25 cycles were performed with 2 µl of the eluted

chromatin samples or input (1:50), PCR products were visualized on 4% TAE agarose gels. *In silico* transcription factor binding site prediction was performed using the Genomatix Software Suite (Munich, Germany) or based on unpublished results of D. Penkow (Lomonosov Moscow State University, Russia).

Statistical analysis

The total number of animals, injected brain hemispheres, technical replicates and number of cells counted per experiment are summarized in supplementary material Tables S3-S5. Standard deviation was calculated between injected hemispheres and technical replicates respectively. Error bars represent s.e.m. Comparison between two groups was performed with unpaired Student's *t*-test, comparison between three or more groups was carried out by one-way ANOVA followed by Tukey's Multiple Comparison post-hoc test (Prism 5.01, Graph Pad). Statistical significance was assumed when $P<0.05$, indicated as $*P<0.05$, $**P<0.01$, $***P<0.001$.

Acknowledgements

We are grateful to D. Anderson (Caltech, Pasadena, USA), A. Buchberg (Thomas Jefferson University, Philadelphia, USA), R. Kageyama (Kyoto University, Kyoto, Japan), D. Engelkamp (University Erlangen-Nürnberg, Germany), L. Selleri (Weill, Cornell Medical College, New York City, USA), Michael L. Cleary (Stanford University, Stanford, USA) and J. Kohtz (Northwestern University, Chicago, USA) for reagents; to Y. Yanagawa (National Institute for Physiological Sciences, Okazaki, Japan) for the GAD::GFP mouse line; to N. Bobola (Manchester University, UK) for experimental advice; and to D. Penkow (Moscow State University, Russia) for help with transcription factor binding site prediction.

Competing interests

The authors declare no competing financial interests.

Author contributions

Z.A., P.H., M.S.B. designed and conducted the experiments, and contributed to writing the manuscript; B.M.G. contributed to the experiments shown in Fig. 4; A.-C.H. contributed to the experiments shown in Fig. 7; W.K.-G. contributed to the experiments shown in Fig. 3; J.S. contributed to the experiments shown in Fig. 6; M.G. designed, discussed and supervised experiments shown in Figs 1,2,4 and 5, and contributed to writing the manuscript; D.S. designed the study, discussed and supervised the experiments, and wrote the manuscript.

Funding

This work was supported by the Deutsche Forschungsgemeinschaft [SCHU 1218/3-1] and the Schram Foundation [T287/21795/2011] (D.S.) and EUTRACC and SFB 870 (M.G.). Z.A. was a recipient of a predoctoral fellowship from the Studienstiftung des Deutschen Volkes.

Supplementary material

Supplementary material available online at
http://dev.biologists.org/lookup/suppl/doi:10.1242/dev.097295/-/DC1

References

Agoston, Z. and Schulte, D. (2009). Meis2 competes with the Groucho co-repressor Tle4 for binding to Otx2 and specifies tectal fate without induction of a secondary midbrain-hindbrain boundary organizer. *Development* **136**, 3311-3322.

Agoston, Z., Li, N., Haslinger, A., Wizenmann, A. and Schulte, D. (2012). Genetic and physical interaction of Meis2, Pax3 and Pax7 during dorsal midbrain development. *BMC Dev. Biol.* **12**, 10.

Allen, Z. J., 2nd, Waclaw, R. R., Colbert, M. C. and Campbell, K. (2007). Molecular identity of olfactory bulb interneurons: transcriptional codes of periglomerular neuron subtypes. *J. Mol. Histol.* **38**, 517-525.

Azcoitia, V., Aracil, M., Martínez-A, C. and Torres, M. (2005). The homeodomain protein Meis1 is essential for definitive hematopoiesis and vascular patterning in the mouse embryo. *Dev. Biol.* **280**, 307-320.

Berger, J., Eckert, S., Scardigli, R., Guillemot, F., Gruss, P. and Stoykova, A. (2004). E1-Ngn2/Cre is a new line for regional activation of Cre recombinase in the developing CNS. *Genesis* **40**, 195-199.

Berkes, C. A., Bergstrom, D. A., Penn, B. H., Seaver, K. J., Knoepfler, P. S. and Tapscott, S. J. (2004). Pbx marks genes for activation by MyoD indicating a role for a homeodomain protein in establishing myogenic potential. *Mol. Cell* **14**, 465-477.

Bessa, J., Tavares, M. J., Santos, J., Kikuta, H., Laplante, M., Becker, T. S., Gómez-Skarmeta, J. L. and Casares, F. (2008). meis1 regulates cyclin D1 and c-myc expression, and controls the proliferation of the multipotent cells in the early developing zebrafish eye. *Development* **135**, 799-803.

Brill, M. S., Snapyan, M., Wohlfrom, H., Ninkovic, J., Jawerka, M., Mastick, G. S., Ashery-Padan, R., Saghatelyan, A., Berninger, B. and Götz, M. (2008). A dlx2- and pax6-dependent transcriptional code for periglomerular neuron specification in the adult olfactory bulb. *J. Neurosci.* **28**, 6439-6452.

Brill, M. S., Ninkovic, J., Winpenny, E., Hodge, R. D., Ozen, I., Yang, R., Lepier, A., Gascón, S., Erdelyi, F., Szabo, G. et al. (2009). Adult generation of glutamatergic olfactory bulb interneurons. *Nat. Neurosci.* **12**, 1524-1533.

Bumsted-O'Brien, K. M., Hendrickson, A., Haverkamp, S., Ashery-Padan, R. and Schulte, D. (2007). Expression of the homeodomain transcription factor Meis2 in the embryonic and postnatal retina. *J. Comp. Neurol.* **505**, 58-72.

Calvo, K. R., Knoepfler, P. S., Sykes, D. B., Pasillas, M. P. and Kamps, M. P. (2001). Meis1a suppresses differentiation by G-CSF and promotes proliferation by SCF: potential mechanisms of cooperativity with Hoxa9 in myeloid leukemia. *Proc. Natl. Acad. Sci. USA* **98**, 13120-13125.

Capellini, T. D., Di Giacomo, G., Salsi, V., Brendolan, A., Ferretti, E., Srivastava, D., Zappavigna, V. and Selleri, L. (2006). Pbx1/Pbx2 requirement for distal limb patterning is mediated by the hierarchical control of Hox gene spatial distribution and Shh expression. *Development* **133**, 2263-2273.

Carbe, C., Hertzler-Schaefer, K. and Zhang, X. (2012). The functional role of the Meis/Prep-binding elements in Pax6 locus during pancreas and eye development. *Dev. Biol.* **363**, 320-329.

Chang, C. P., Jacobs, Y., Nakamura, T., Jenkins, N. A., Copeland, N. G. and Cleary, M. L. (1997). Meis proteins are major in vivo DNA binding partners for wild-type but not chimeric Pbx proteins. *Mol. Cell. Biol.* **17**, 5679-5687.

Choe, S. K., Lu, P., Nakamura, M., Lee, J. and Sagerström, C. G. (2009). Meis cofactors control HDAC and CBP accessibility at Hox-regulated promoters during zebrafish embryogenesis. *Dev. Cell* **17**, 561-567.

De Marchis, S., Bovetti, S., Carletti, B., Hsieh, Y. C., Garzotto, D., Peretto, P., Fasolo, A., Puche, A. C. and Rossi, F. (2007). Generation of distinct types of periglomerular olfactory bulb interneurons during development and in adult mice: implication for intrinsic properties of the subventricular zone progenitor population. *J. Neurosci.* **27**, 657-664.

de Melo, J., Qiu, X., Du, G., Cristante, L. and Eisenstat, D. D. (2003). Dlx1, Dlx2, Pax6, Brn3b, and Chx10 homeobox gene expression defines the retinal ganglion and inner nuclear layers of the developing and adult mouse retina. *J. Comp. Neurol.* **461**, 187-204.

Dyer, B.W., Ferrer, F.A., Klinedinst, D.K. and Rodriguez, R. (2000). A noncommercial dual luciferase enzyme assay system for reporter gene analysis. *Anal. Biochem.* **282**, 158-161.

Elkouby, Y. M., Polevoy, H., Gutkovich, Y. E., Michaelov, A. and Frank, D. (2012). A hindbrain-repressive Wnt3a/Meis3/Tsh1 circuit promotes neuronal differentiation and coordinates tissue maturation. *Development* **139**, 1487-1497.

Engelkamp, D., Rashbass, P., Seawright, A. and van Heyningen, V. (1999). Role of Pax6 in development of the cerebellar system. *Development* **126**, 3585-3596.

Epstein, J. A., Glaser, T., Cai, J., Jepeal, L., Walton, D. S. and Maas, R. L. (1994). Two independent and interactive DNA-binding subdomains of the Pax6 paired domain are regulated by alternative splicing. *Genes Dev.* **8**, 2022-2034.

Francis, F., Koulakoff, A., Boucher, D., Chafey, P., Schaar, B., Vinet, M. C., Friocourt, G., McDonnell, N., Reiner, O., Kahn, A. et al. (1999). Doublecortin is a developmentally regulated, microtubule-associated protein expressed in migrating and differentiating neurons. *Neuron* **23**, 247-256.

Gleeson, J. G., Lin, P. T., Flanagan, L. A. and Walsh, C. A. (1999). Doublecortin is a microtubule-associated protein and is expressed widely by migrating neurons. *Neuron* **23**, 257-271.

Hack, M. A., Saghatelyan, A., de Chevigny, A., Pfeifer, A., Ashery-Padan, R., Lledo, P. M. and Götz, M. (2005). Neuronal fate determinants of adult olfactory bulb neurogenesis. *Nat. Neurosci.* **8**, 865-872.

Haubst, N., Berger, J., Radjendirane, V., Graw, J., Favor, J., Saunders, G. F., Stoykova, A. and Götz, M. (2004). Molecular dissection of Pax6 function: the specific roles of the paired domain and homeodomain in brain development. *Development* **131**, 6131-6140.

Heanue, T. A., Reshef, R., Davis, R. J., Mardon, G., Oliver, G., Tomarev, S., Lassar, A. B. and Tabin, C. J. (1999). Synergistic regulation of vertebrate muscle development by Dach2, Eya2, and Six1, homologs of genes required for Drosophila eye formation. *Genes Dev.* **13**, 3231-3243.

Heine, P., Dohle, E., Bumsted-O'Brien, K., Engelkamp, D. and Schulte, D. (2008). Evidence for an evolutionary conserved role of homothorax/Meis1/2 during vertebrate retina development. *Development* **135**, 805-811.

Hisa, T., Spence, S. E., Rachel, R. A., Fujita, M., Nakamura, T., Ward, J. M., Devor-Henneman, D. E., Saiki, Y., Kutsuna, H., Tessarollo, L. et al. (2004). Hematopoietic, angiogenic and eye defects in Meis1 mutant animals. *EMBO J.* **23**, 450-459.

Hojo, M., Ohtsuha, T., Hashimoto, N., Gradwohl, G., Guillemot, F. and Kageyama, R. (2000). Glial cell fate specification modulated by the bHLH gene Hes5 in mouse retina. *Development* **127**, 2515-2522.

Hsieh, J. (2012). Orchestrating transcriptional control of adult neurogenesis. *Genes Dev.* **26**, 1010-1021.

Hyman-Walsh, C., Bjerke, G. A. and Wotton, D. (2010). An autoinhibitory effect of the homothorax domain of Meis2. *FEBS J.* **277**, 2584-2597.

Karl, C., Couillard-Despres, S., Prang, P., Munding, M., Kilb, W., Brigadski, T., Plötz, S., Mages, W., Luhmann, H., Winkler, J. et al. (2005). Neuronal precursor-specific activity of a human doublecortin regulatory sequence. *J. Neurochem.* **92**, 264-282.

Kleinjan, D. A., Seawright, A., Childs, A. J. and van Heyningen, V. (2004). Conserved elements in Pax6 intron 7 involved in (auto)regulation and alternative transcription. *Dev. Biol.* **265**, 462-477.

Knoepfler, P. S., Bergstrom, D. A., Uetsuki, T., Dac-Korytko, I., Sun, Y. H., Wright, W. E., Tapscott, S. J. and Kamps, M. P. (1999). A conserved motif N-terminal to the DNA-binding domains of myogenic bHLH transcription factors mediates cooperative DNA binding with pbx-Meis1/Prep1. *Nucleic Acids Res.* **27**, 3752-3767.

Kohwi, M., Osumi, N., Rubenstein, J. L. and Alvarez-Buylla, A. (2005). Pax6 is required for making specific subpopulations of granule and periglomerular neurons in the olfactory bulb. *J. Neurosci.* **25**, 6997-7003.

Kohwi, M., Petryniak, M. A., Long, J. E., Ekker, M., Obata, K., Yanagawa, Y., Rubenstein, J. L. and Alvarez-Buylla, A. (2007). A subpopulation of olfactory bulb GABAergic interneurons is derived from Emx1- and Dlx5/6-expressing progenitors. *J. Neurosci.* **27**, 6878-6891.

Kozmik, Z., Czerny, T. and Busslinger, M. (1997). Alternatively spliced insertions in the paired domain restrict the DNA sequence specificity of Pax6 and Pax8. *EMBO J.* **16**, 6793-6803.

Kutejova, E., Engist, B., Self, M., Oliver, G., Kirilenko, P. and Bobola, N. (2008). Six2 functions redundantly immediately downstream of Hoxa2. *Development* **135**, 1463-1470.

Maeda, R., Ishimura, A., Mood, K., Park, E. K., Buchberg, A. M. and Daar, I. O. (2002). Xpbx1b and Xmeis1b play a collaborative role in hindbrain and neural crest gene expression in Xenopus embryos. *Proc. Natl. Acad. Sci. USA* **99**, 5448-5453.

Marei, H. E., Ahmed, A. E., Michetti, F., Pescatori, M., Pallini, R., Casalbore, P., Cenciarelli, C. and Elhadidy, M. (2012). Gene expression profile of adult human olfactory bulb and embryonic neural stem cell suggests distinct signaling pathways and epigenetic control. *PLoS ONE* **7**, e33542.

Mendoza-Torreblanca, J. G., Martínez-Martínez, E., Tapia-Rodríguez, M., Ramírez-Hernández, R. and Gutiérrez-Ospina, G. (2008). The rostral migratory stream is a neurogenic niche that predominantly engenders periglomerular cells: in vivo evidence in the adult rat brain. *Neurosci. Res.* **60**, 289-299.

Mercader, N., Leonardo, E., Azpiazu, N., Serrano, A., Morata, G., Martínez, C. and Torres, M. (1999). Conserved regulation of proximodistal limb axis development by Meis1/Hth. *Nature* **402**, 425-429.

Merkle, F. T., Mirzadeh, Z. and Alvarez-Buylla, A. (2007). Mosaic organization of neural stem cells in the adult brain. *Science* **317**, 381-384.

Mishra, R., Gorlov, I. P., Chao, L. Y., Singh, S. and Saunders, G. F. (2002). PAX6, paired domain influences sequence recognition by the homeodomain. *J. Biol. Chem.* **277**, 49488-49494.

Moens, C. B. and Selleri, L. (2006). Hox cofactors in vertebrate development. *Dev. Biol.* **291**, 193-206.

Moskow, J. J., Bullrich, F., Huebner, K., Daar, I. O. and Buchberg, A. M. (1995). Meis1, a PBX1-related homeobox gene involved in myeloid leukemia in BXH-2 mice. *Mol. Cell. Biol.* **15**, 5434-5443.

Mu, L., Berti, L., Masserdotti, G., Covic, M., Michaelidis, T. M., Doberauer, K., Merz, K., Rehfeld, F., Haslinger, A., Wegner, M. et al. (2012). SoxC transcription factors are required for neuronal differentiation in adult hippocampal neurogenesis. *J. Neurosci.* **32**, 3067-3080.

Nakamura, T., Jenkins, N. A. and Copeland, N. G. (1996). Identification of a new family of Pbx-related homeobox genes. *Oncogene* **13**, 2235-2242.

Ortega, F., Gascón, S., Masserdotti, G., Deshpande, A., Simon, C., Fischer, J., Dimou, L., Chichung Lie, D., Schroeder, T. and Berninger, B. (2013). Oligodendrogliogenic and neurogenic adult subependymal zone neural stem cells constitute distinct lineages and exhibit differential responsiveness to Wnt signalling. *Nat. Cell Biol.* **15**, 602-613.

Paige, S. L., Thomas, S., Stoick-Cooper, C. L., Wang, H., Maves, L., Sandstrom, R., Pabon, L., Reinecke, H., Pratt, G., Keller, G. et al. (2012). A temporal chromatin signature in human embryonic stem cells identifies regulators of cardiac development. *Cell* **151**, 221-232.

Parmar, M., Sjöberg, A., Björklund, A. and Kokaia, Z. (2003). Phenotypic and molecular identity of cells in the adult subventricular zone. in vivo and after expansion in vitro. *Mol. Cell. Neurosci.* **24**, 741-752.

Parrish-Aungst, S., Shipley, M. T., Erdelyi, F., Szabo, G. and Puche, A. C. (2007). Quantitative analysis of neuronal diversity in the mouse olfactory bulb. *J. Comp. Neurol.* **501**, 825-836.

Penkov, D., Mateos San Martín, D., Fernandez-Días, L.C., Rosselló, C.A., Torroja, C., Sánchez-Cabo, F., Warnatz, H.J., Sultan, M., Yaspo, M.L. et al. (2013). Analysis of the DNA-binding profile and function of TALE homeoproteins reveals their specialization and specific interactions with Hox genes/proteins. *Cell Rep.* **3**, 1321-1333.

Pennartz, S., Belvindrah, R., Tomiuk, S., Zimmer, C., Hofmann, K., Conradt, M., Bosio, A. and Cremer, H. (2004). Purification of neuronal precursors from the adult mouse brain: comprehensive gene expression analysis provides new insights into the control of cell migration, differentiation, and homeostasis. *Mol. Cell. Neurosci.* **25**, 692-706.

Piens, M., Muller, M., Bodson, M., Baudouin, G. and Plumier, J. C. (2010). A short upstream promoter region mediates transcriptional regulation of the mouse doublecortin gene in differentiating neurons. *BMC Neurosci.* **11**, 64.

Rave-Harel, N., Givens, M. L., Nelson, S. B., Duong, H. A., Coss, D., Clark, M. E., Hall, S. B., Kamps, M. P. and Mellon, P. L. (2004). TALE homeodomain proteins regulate gonadotropin-releasing hormone gene expression independently and via interactions with Oct-1. *J. Biol. Chem.* **279**, 30287-30297.

Reynolds, B. A. and Weiss, S. (1992). Generation of neurons and astrocytes from isolated cells of the adult mammalian central nervous system. *Science* **255**, 1707-1710.

Royo, J. L., Bessa, J., Hidalgo, C., Fernández-Miñán, A., Tena, J. J., Roncero, Y., Gómez-Skarmeta, J. L. and Casares, F. (2012). Identification and analysis of conserved cis-regulatory regions of the MEIS1 gene. *PLoS ONE* **7**, e33617.

Singh, S., Mishra, R., Arango, N. A., Deng, J. M., Behringer, R. R. and Saunders, G. F. (2002). Iris hypoplasia in mice that lack the alternatively spliced Pax6(5a) isoform. *Proc. Natl. Acad. Sci. USA* **99**, 6812-6815.

Tamamaki, N., Yanagawa, Y., Tomioka, R., Miyazaki, J., Obata, K. and Kaneko, T. (2003). Green fluorescent protein expression and colocalization with calretinin, parvalbumin, and somatostatin in the GAD67-GFP knock-in mouse. *J. Comp. Neurol.* **467**, 60-79.

Vitobello, A., Ferretti, E., Lampe, X., Vilain, N., Ducret, S., Ori, M., Spetz, J. F., Selleri, L. and Rijli, F. M. (2011). Hox and Pbx factors control retinoic acid synthesis during hindbrain segmentation. *Dev. Cell* **20**, 469-482.

Vlachakis, N., Choe, S. K. and Sagerström, C. G. (2001). Meis3 synergizes with Pbx4 and Hoxb1b in promoting hindbrain fates in the zebrafish. *Development* **128**, 1299-1312.

Waclaw, R. R., Allen, Z. J., 2nd, Bell, S. M., Erdélyi, F., Szabó, G., Potter, S. S. and Campbell, K. (2006). The zinc finger transcription factor Sp8 regulates the generation and diversity of olfactory bulb interneurons. *Neuron* **49**, 503-516.

Walcher, T., Xie, Q., Sun, J., Irmler, M., Beckers, J., Öztürk, T., Niessing, D., Stoykova, A., Cvekl, A., Ninkovic, J. et al. (2013). Functional dissection of the paired domain of Pax6 reveals molecular mechanisms of coordinating neurogenesis and proliferation. *Development* **140**, 1123-1136.

Wassef, M. A., Chomette, D., Pouilhe, M., Stedman, A., Havis, E., Desmarquet-Trin Dinh, C., Schneider-Maunoury, S., Gilardi-Hebenstreit, P., Charnay, P. and Ghislain, J. (2008). Rostral hindbrain patterning involves the direct activation of a Krox20 transcriptional enhancer by Hox/Pbx and Meis factors. *Development* **135**, 3369-3378.

Wong, P., Iwasaki, M., Somervaille, T. C., So, C. W. and Cleary, M. L. (2007). Meis1 is an essential and rate-limiting regulator of MLL leukemia stem cell potential. *Genes Dev.* **21**, 2762-2774.

Zhang, X., Friedman, A., Heaney, S., Purcell, P. and Maas, R. L. (2002). Meis homeoproteins directly regulate Pax6 during vertebrate lens morphogenesis. *Genes Dev.* **16**, 2097-2107.

Zhang, X., Rowan, S., Yue, Y., Heaney, S., Pan, Y., Brendolan, A., Selleri, L. and Maas, R. L. (2006). Pax6 is regulated by Meis and Pbx homeoproteins during pancreatic development. *Dev. Biol.* **300**, 748-757.

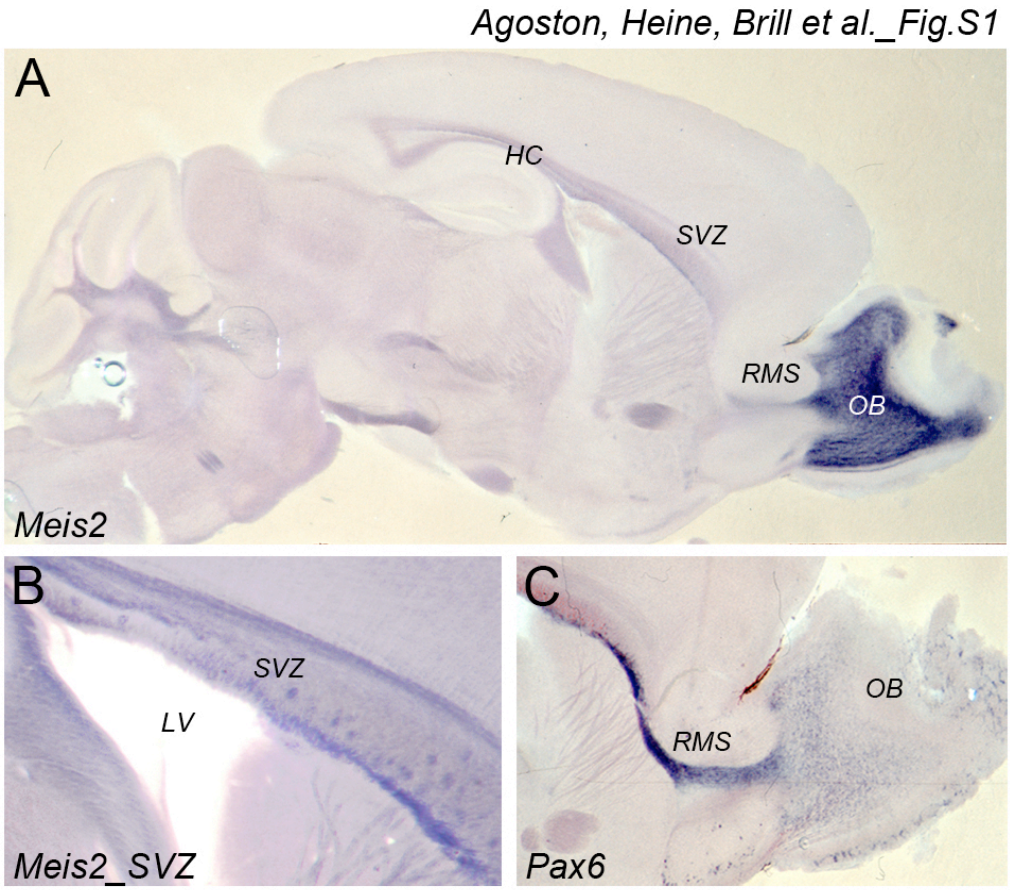

Supporting Figure 1: *Meis2* and *Pax6* transcripts in the adult murine brain detected by in situ hybridization on vibratome sections. (A) *Meis2*-specific transcripts on a sagittal section through the brain of a 7 week old mouse; strong expression is detectable in the SVZ-OB neurogenic system. (B) *Meis2*-mRNA in the SVZ. (C) *Pax6* specific transcripts in the SVZ, RMS and OB. Cells in the glomerular layer and neuroblasts that migrate from the RMS laterally into the outer olfactory bulb express *Pax6*. [HC: hippocampus; LV: lateral ventricle; OB: olfactory bulb; RMS: rostral migratory stream; SVZ: subventricular zone]

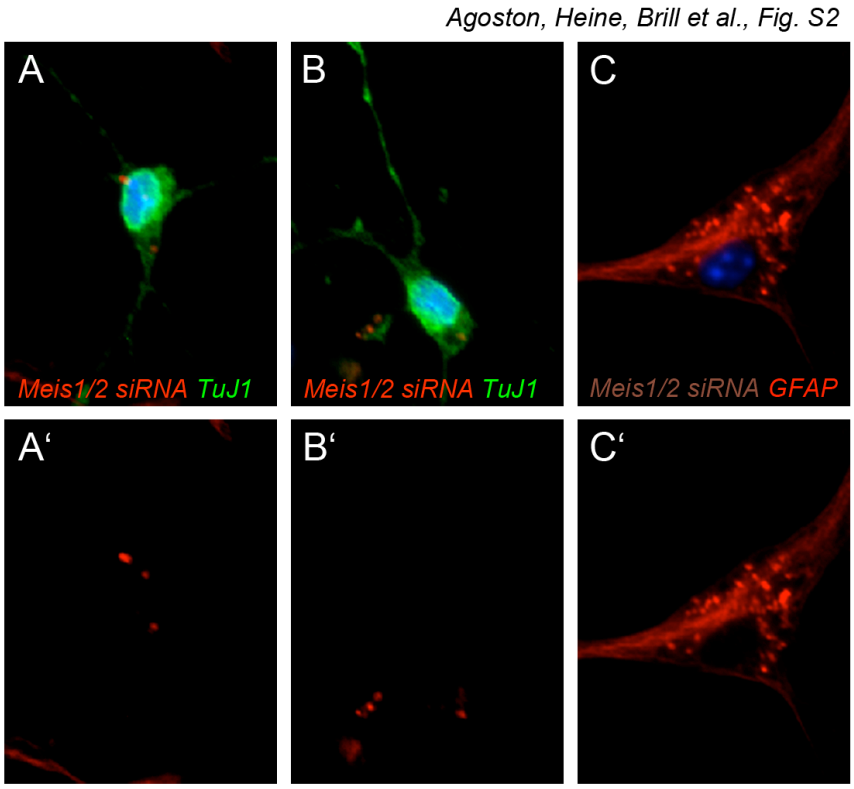

Supporting Figure 2. Representative examples of neurosphere cells that were transfected with siRNAs specific for *Meis1* and *Meis2* and allowed to differentiate in vitro for two days. (A, B): cells stained for TuJ1 (green, detected with an Alexa488-coupled secondary antibody); (C) cell stained for GFAP (red, detected with an Alexa594-coupled secondary antibody). The rare TuJ1-expressing neurons generated from *Meis1/2 siRNA* transfected cells exhibited markedly fewer red-fluorescent speckles (indicative of lower uptake of the Cy5-labeled siRNA molecules) than astrocytes generated from *Meis1/2 siRNA* transfected cells. In (A'), (B') and (C') only the red channel is shown for clarity. The fluorescent signals of GFAP and *Meis1/2 siRNA* overlap in (C, C').

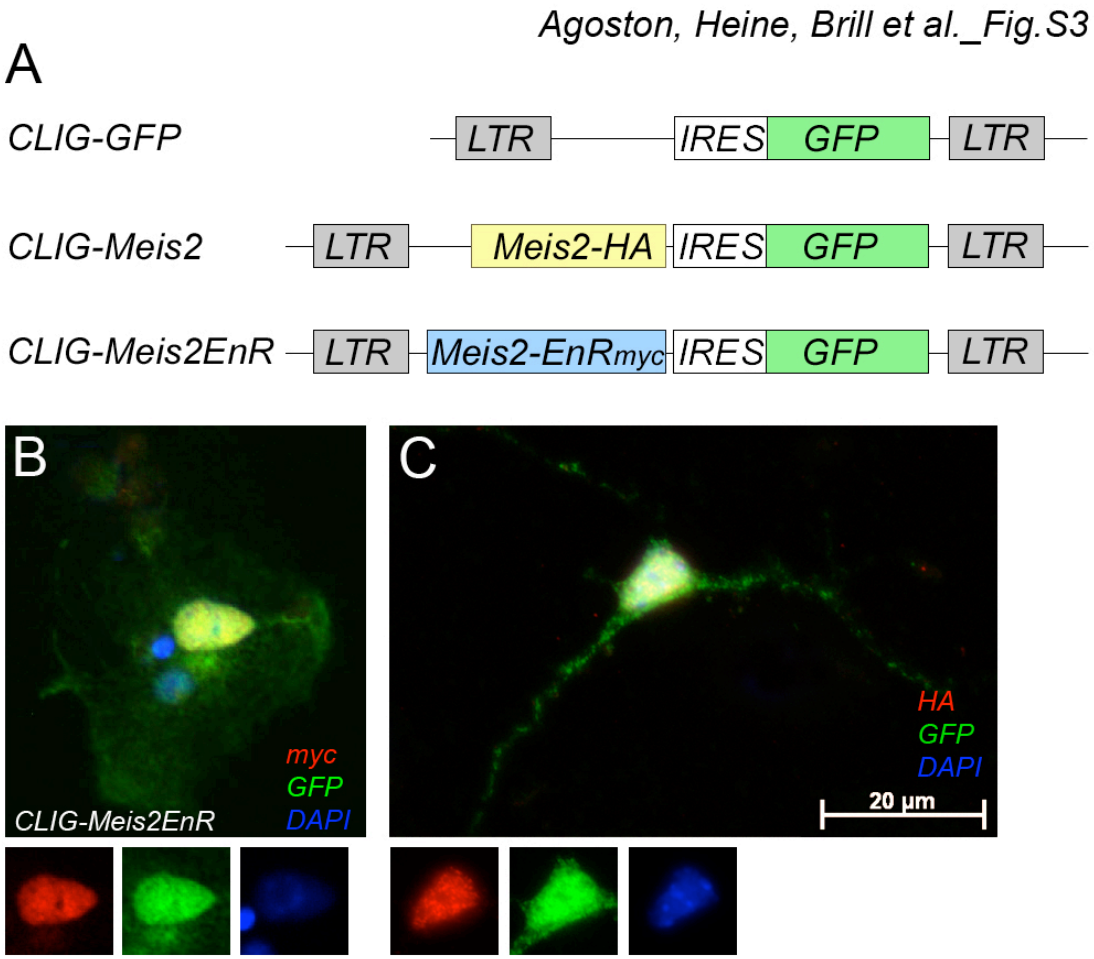

Supporting Figure 3. Schematic representation of the retroviral construct used in this study. (A) All CLIG-derived retroviral vectors express GFP from an internal ribosome entry site (IRES). CLIG-Meis2 contains *Meis2a* C-terminally fused to a triple HA-epitope, CLIG-Meis2EnR contains *Meis2a* fused to the EnR domain of *D. melanogaster* and a single C-terminal myc-epitope. (B, C) Co-expression of GFP with the transgenes in CLIG-Meis2 and CLIG-Meis2EnR. (B) An in vitro differentiated, neurosphere derived cell infected with Meis2EnR exhibits GFP- and nuclear myc staining. (C) An in vitro differentiated, neurosphere derived cell infected with Meis2HA exhibits GFP- and nuclear HA staining.

Agoston, Heine, Brill et al._Fig. S4

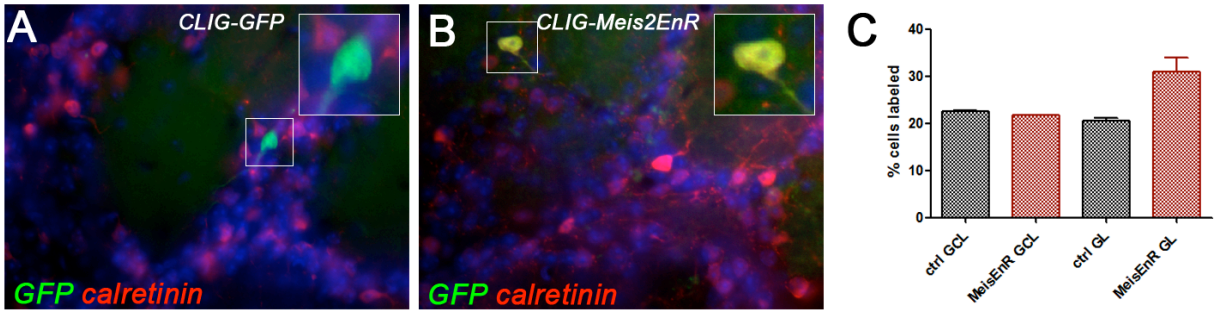

Supporting Figure 4. Some Meis2EnR transduced periglomerular neurons acquire a calretinin-positive PGN fate. Images were taken 21 days after the CLIG-GFP control virus or CLIG-Meis2EnR were injected into the RMS, (A) Representative example of a GFP transduced PGN (green) not immunoreactive for calretinin (red); (B) Representative example of a Meis2EnR transduced PGN (green) expressing calretinin (green). (C) Quantification of the results.

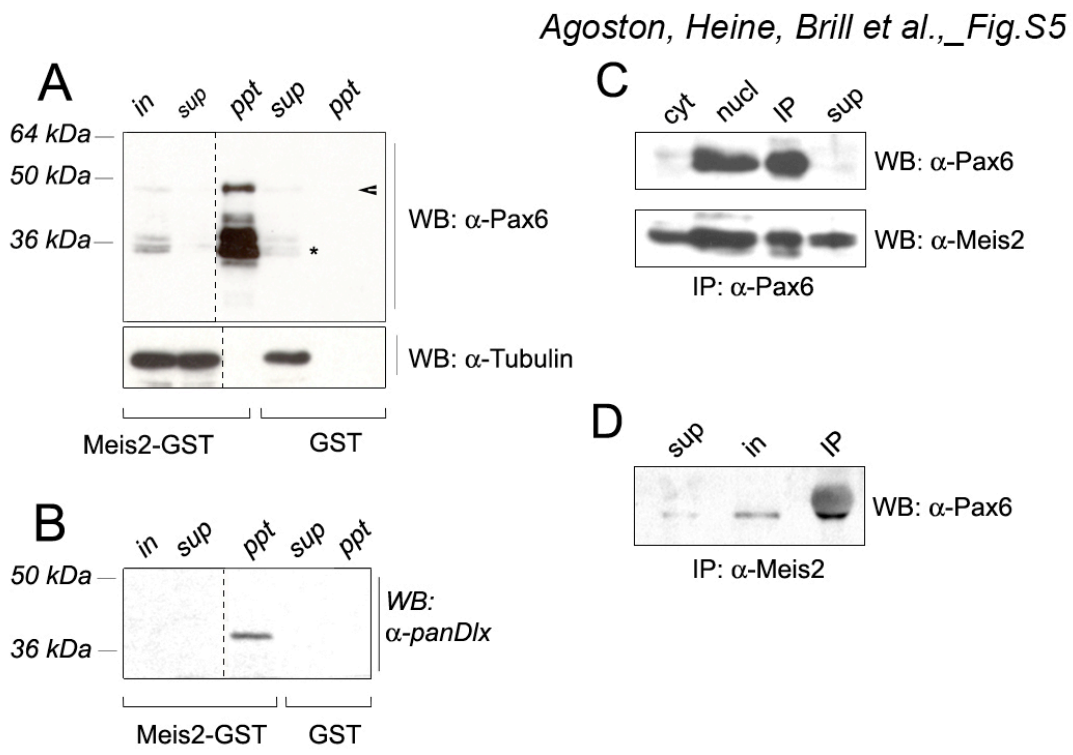

Supporting Figure 5. Meis2-Dlx2-Pax6 containing protein complexes exist in the embryonic chick eye. (A) GST pull-down with Meis2-GST or GST alone and protein extracts from HH (Hamburger Hamilton stage) 15-17 embryonic chick eyes. Top panel: Western blot with a Pax6 specific antibody; bottom panel: Western blot with α-tubulin as control. (B) Same blot as in (A) but re-probed with an antibody with broad specificity for Dlx proteins. Dlx can be enriched by Meis2-GST but not GST alone. The dashed lines indicate that the blot was cut to remove the marker lane. (C) Immunoprecipitation from chick eye extracts with a mouse monoclonal antibody directed against Pax6. Top panel: Western blot with a rabbit polyclonal Pax6-antibody; bottom panel: the same blot as above but re-probed with a rabbit polyclonal antibody specific for Meis2. Meis2 can be successfully co-precipitated with the Pax6. (D) Immunoprecipitation from chick eye extracts with a rabbit polyclonal antibody directed against Meis2. Western blot with a mouse monoclonal Pax6-antibody reveals association of Pax6 with Meis2. [*in*: input; *sup*: supernatant; *ppt*: precipitate of the pull-down; *IP*: immunoprecipitate]

Supporting Figure 6. Sequence of genomic region upstream of the DCX translational start, which was analyzed in the present study; putative transcription factor binding sites are highlighted: Meis/Pbx (red), Pax4/6 (blue), Dlx (green); + and - indicate location of the consensus binding site on the coding or non coding strand; putative CAAT- and TATAA-boxes are underlined; the location of the primers used for ChIP-qPCR are italicized and marked by arrows.

Table S1: Antibodies

Primary antibodies for immunohistochemistry and Western Blot			
name	**species**	**source**	**dilution**
anti-calbindin	mouse	Sigma Immunochemicals, Germany, C9848	1:1000
anti-calretinin	mouse	BD Biosciences, Franklin Lakes, NJ, 610908	1:2000
anti-pan-Dlx	rabbit	J. Kohtz, Children's Memorial Hospital and Feinberg School of Medicine, Northwestern University, Chicago, IL	1:750
anti-doublecortin (DCX)	guinea pig	Millipore Bioscience Research Reagents, Billerica, MA, AB2253	1:2000
anti-doublecortin (DCX)	rabbit	Abcam, Cambridge, MA, ab18723	1:2000
anti-GFAP	mouse	Sigma Immunochemicals, Germany, G 9269	1:500
anti-GFP	rabbit	Molecular Probes, OR	1:5000
anti-glutamate decarboxylase 67kDa (GAD67)	mouse	Millipore, MAB5406	1:1000
anti-HA	rat	Roche Diagnostics, Germany, 3F10	1:1000
anti-Ascl1 (Mash1)	mouse	D. Anderson, California Institute of Technology, Pasadena, CA	1:200
anti-Meis2	rabbit	A. Buchberg, Kimmel Cancer Centre, University of Philadelphia Medical School	1:5000
anti-Meis2	mouse	Sigma Immunochemicals, clone 1H4	1:1000
anti-myc	mouse	Abcam, Cambridge, MA, ab11917	1:100
anti-Olig2	rabbit	Millipore Bioscience Research Reagents, Billerica, MA, AB9610	1:1000
anti-O4	mouse	hybridoma supernatant; M. Schachner, Center for Molecular Neurobiology, Hamburg, Germany	1:5
anti-Pax6	mouse	Developmental Studies Hybridoma Bank, IA	Purified IgGs: 1:5000 or hybridoma supernatant 1:10
anti-Pax6	mouse	clone AB2.38 of (Engelkamp et al., 1999, Development 126(16):3585-96.	Purified IgGs: 1:5000 for Western Blots or supernatant

			1:10
anti- Pax6	rabbit	Covance, Princeton, NJ, PRB-278P	1:1000 for Western Blots
anti-PSA-NCAM ,	mouse	Millipore Bioscience Research Reagents, Billerica, MA, MAB5324	1:1000
anti-tubulin, isotype III, (TuJ1)	mouse	Covance, Princeton, NJ, MMS435P	1:1000
anti-tyrosine hydroxylase (TH)	mouse	Millipore Bioscience Research Reagents, MAB5280	1:500
Antibodies for ChIP			
name	**species**	**source**	
anti-Meis2 N-17X	goat	Santa Cruz Biotechnology, Santa Cruz, CA, sc-10600	
anti-Pax6	mouse	purified IgGs, Developmental Studies Hybridoma Bank, IA	
anti-pan-Dlx	rabbit	J. Kohtz, Northwestern University, Chicago, IL	
anti-RNA Pol II	mouse	Merck Millipore, Germany, clone CTD4H8	
Normal IgG control	mouse	Merck Millipore / Upstate, # 12-371B from EZ-ChIP Kit # 17-371	

Secondary antibodies for immunohistochemistry were Alexa 594-, Alexa 488-, Cy2 or Cy3 conjugated (Molecular Probes, OR, Invitrogen, Karlsruhe, Germany or Dianova, Hamburg, Germany). Some sections were counterstained with 4'-6-Diamidino-2-phenylindole (DAPI) to visualize cell nuclei. Stainings were analyzed with either a LSM5 confocal microscope (Zeiss, Germany), an Axioplan2 with deconvolution software, or an Olympus FV1000 laser-scanning confocal microscope with optical sections of maximum 1–2 μm intervals.

Table S2: Primer Sequences for ChIP

name	sequence	amplicon
DCXI for	5'- CTCGGATACTTCACTCAGTATATC	
DCXI rev	5'- GCATATCTGTGTTTATGGCTGC	178bp
DCXII for	5'- AAACCTTTCTAGCTGTTAATGCAGG	
DCXII rev	5'- CTCCAAGCAAGAAATTCCTGCCAGGGTG	174bp
TH1 for	5'- CCTCTTTAGTTTCCTGATGTCCTGG	
TH1 rev	5'- GCCTGTGGAGCAGGCAACAGAAGG	192bp
TH2 for	5'- GTCTCCTGTCCCAGAACACCAGCC	
TH2 rev	5'- TAAAGGCCAGGCTGACGTCAAAGC	245bp
GAPDH	#PP1045500, Diagenode, Liège, Belgium	
Myogenin for	5'- CAAATTACAGCCGACGGCCTC	
Myogenin rev	5-' GAAAAGGCTTGTTCCTGCCACTG	284bp

Table S3: Total number of Meis2-immunreactive cells in the SVZ, RMS and OB analyzed

antigen	**% of cells co-labeled with Meis2**	**total number of cell counted**
SVZ/RMS		
DCX	98.7%	1678 cells, 3 animals
TuJ1	95.1%	870 cells, 3 animals
PSA-NCAM	99.3%	772 cells, 3 animals
OB		
tyrosine hydroxylase, TH	94.4% (+/- 3.1%)	1913 cells, 3 animals
calbindin	62.9% (+/- 2.1%)	2571 cells, 4 animals
calretinin	28.3% (+/- 1.4%)	2121 cells, 3 animals
Pax6	83.5% (+/- 2.5%)	1010 cells, 3 animals
GAD67:GFP	86.8% (+/- 3.7%)	3287 cells, 3 animals
BrdU (3w pulse, 3w chase)	GCL: 87.5% GL: 57.3%	GCL: 512 cells, 1 animal GL: 128 cells, 1 animal

Table S4: Total number of number of cells analyzed following differentiation of neurosphere cells in vitro

A: in vitro differentiation of neurosphere cells following siRNA mediated knock-down

experimental design	number of independent experiments	total number of cell counted
ctrl. siRNA	3	1820
Meis1/2 siRNA	3	1645

B: in vitro differentiation of neurosphere cells following retroviral transduction

experimental design: viral vector / marker / differentiation duration	number of independent experiments	% cells generated	total number of cell counted
CLIG-GFP/ TuJ1 / 3d differentiation	6	11.48 (+/- 0.297 s.e.m.)	3185
CLIG-GFP/ GFAP / 3d differentiation	6	48.44 (+/- 6.28 s.e.m.)	3030
CLIG-Meis2HA/ TuJ1 / 3d differentiation	3	11.39 (+/- 0.695 s.e.m.)	3475
CLIG-Meis2HA/ GFAP / 3d differentiation	3	32.96 (+/- 0.1 s.e.m)	3521
CLIG-Meis2EnR/ TuJ1 / 3d differentiation	3	6.51 (+/- 0.178 s.e.m.)	3219
CLIG-Meis2EnR/ GFAP / 3d differentiation	3	52.19 (+/- 8.50 s.e.m.)	2780
CLIG-GFP/ TuJ1 / 7d differentiation	7	32.49 (+/- 4.37 s.e.m.)	1944
CLIG-GFP/ GFAP / 7d differentiation	3	49.37 (+/- 0.61 s.e.m.)	2126
CLIG-GFP/ O4 / 7d differentiation	3	4.38 (+/- 0.53 s.e.m.)	1391
CLIG-Meis2HA/ TuJ1 / 7d differentiation	3	26.7 (+/- 10.37 s.e.m.)	1807
CLIG-Meis2HA/ GFAP / 7d differentiation	3	53.03 (+/- 1.92 s.e.m.)	1716
CLIG-Meis2HA/ O4 / 7d differentiation	3	7.98 (+/- 0.695 s.e.m.)	1082
CLIG-Meis2EnR/ TuJ1 / 7d differentiation	5	10.99 (+/- 2.53 s.e.m.)	1853
CLIG-Meis2EnR/ GFAP / 7d differentiation	3	64.54 (+/- 1.9 s.e.m.)	1535
CLIG-Meis2EnR/ O4 / 7d differentiation	3	5.485 (+/- 0.665 s.e.m.)	1034

Table S5: Total number of cells counted following in vivo transduction

experimental design: viral vector / injection site / days post injection / marker	**number of injected brain hemispheres**	**total number of cell counted**
CLIG-GFP, SVZ, 3d, PSA-NCAM	4	177
CLIG-Meis2, SVZ, 3d, PSA-NCAM	4	104
CLIG-Meis2EnR, SVZ, 3d, PSA-NCAM	6	132
CLIG-GFP, SVZ, 4d, GFAP	4	963
CLIG-Meis2EnR, SVZ 4d GFAP	6	336
CLIG-GFP, SVZ, 10d, GFAP	2	113
CLIG-Meis2EnR, SVZ 10d GFAP	4	30
CLIG-GFP, RMS, 21d, Pax6	4	571
CLIG-Meis2EnR, RMS, 21d, Pax6	4	98
CLIG-GFP, RMS, 21d, TH	4	462
CLIG-Meis2, RMS, 21d, TH	4	109
CLIG-Meis2EnR, RMS, 21d, TH	7	246
CLIG-GFP, RMS, 60d, TH	4	312
CLIG-Meis2, RMS, 60d, TH	5	153
CLIG-Meis2EnR, RMS, 60d, TH	5	88
CLIG-Meis2EnR, RMS, 21d, Nestin	4	105
CLIG-Meis2EnR, RMS, 21d, TuJ1	4	44
CLIG-GFP, RMS, 21d, GAD67	4	225
CLIG-Meis2EnR, RMS, 21d, GAD67	4	172
CLIG-GFP, RMS, 21d, calretinin	2	168
CLIG-Meis2EnR, RMS, 21d, calretinin	2	128
CLIG-GFP, RMS, 21d, calbindin	2	107
CLIG-Meis2EnR, RMS, 21d, calbindin	2	85